Modelling of Ship Superstructure Icing

Application to Ice Bridge Simulators

Ryoji Kato

MASTER THESIS

Title:	Delivered:
Modelling of Ship Superstructure Icing - Application to Ice Bridge Simulator -	10.06.2012
	Availability:
	Open

Student:	Number of pages:
Ryoji Kato	75

Abstract:

Increasing activities on high north regions bring about a demand of safety ship navigation. Under severe weather condition considerable amounts of ice may accumulate on marine structures. Ice bridge simulator is of importance in terms of training for qualified maritime personal. The new ice module to fit for additional problem for the ship icing is introduced with low reality into bridge simulator. Regarding this our aim is to develop ice model that calculate ice load on the ship structure and stability change include parameters of air temperature, relative wind speed, wave height etc. As a result of literature survey theoretical and empirical method with its algorithm is studied. The ice thickness on cylinder and plate as a representative element of the structures are calculated as a function of liquid water content, relative wind speed and freezing fraction for simplified ship superstructures to include the effect of trapped water on deck. Since we have to deal with several thousand of element to be calculated every seconds including iteration process, computer should be used, hence new ice model is proposed by using computer language C++. In case study 300 tonnage size coast guard vessel is selected as a model ship. Under assumptions that those external parameters are stable in the duration of simulation, proposed model is validated. As a result proposed model could simulate total ice load and following stability change, with error of rolling period after 20 hours simulation being 0.14 sec compared to full scale measurement.

Keyword:
Ship superstructure icing
Computer programming
Ice Bridge Simulator

Advisor:

Prof. Egil Pedersen

I

NTNU – Trondheim
Norwegian University of
Science and Technology

Master Thesis

Spring 2012

for

Ryoji Kato

Modeling of Ship Superstructure Icing

- Application to Ice Bridge Simulator -

The Arctic region represents a challenging environment for maritime operations due to polar lows with fast changing winds, drifting ice, icing, and limited visibility. Safety of maritime operations are also affected by lack of high-quality nautical charts, reduced availability for communication, lower quality of weather forecasts and remoteness with lack of emergency response infrastructure.

Norwegians have traditionally been operating ships in Arctic waters as fishermen, seal and whale hunters. The coast guard has long operational experience in the high north, and in recent years there has been a growing activity with vessel operations due to research, cruise traffic, oil and gas exploration. The operators of fishery, petroleum and shipping activities in the high north must take precautions to reduce the level of risk of their operations as an accident can have serious consequences.

Safe operations of ships in the high north require proper design, equipment, planning and knowledge in how to handle a ship when experiencing icing conditions. This thesis shall investigate application of modelling of icing on a ship's superstructure with emphasis on proposing a framework for implementation on a ship handling simulator. The work shall include, but is not limited to, the following:

- A literature survey on existing icing models.
- Development of an icing model that includes major parameters important to the build-up of ice.
- Application of proposed icing model to include the effect of trapped water on deck.
- Case studies with simplified superstructures for assessment of the potential of proposed model.

In the thesis the candidate shall present his/her personal contribution to the resolution of problem within the scope of the thesis work. Theories and conclusions should be based on mathematical derivations and/or logic reasoning identifying the various steps in the deduction. The candidate should utilize the existing possibilities for obtaining relevant literature.

The manuscript should be typed single-sided in Times New Roman font style. Every sheet shall be numbered and arranged according to: Title and subtitle (if desired), the text defining the scope, abstract, acknowledgements (if any), nomenclature and conventions (if any), contents, main body of thesis (suitably divided in numbered main chapters with titles, numbered sub-paragraphs for which further headings are optional), conclusions with recommendations for further work, references and appendices (if appropriate). All figures, tables and equations shall be numerated.

The thesis should be organized in a rational manner to give a clear exposition of results, assessments, and conclusions. The text should be written as concisely as possible, but not at the expense of clarity. Descriptive or explanatory passages, necessary as information but which tend to break up the flow of the text, should be put into appendices. Units and symbols should conform to the recommendations contained in the International System of Units (SI). The thesis should in general not exceed 100 pages.

The supervisor may require that the candidate, in an early stage of the work, present a written plan for the completion of the work. The plan should include a budget for the use of any computer and laboratory resources that will be required and charged to the department. Overruns shall be reported to the supervisor.

The original contribution of the candidate and material taken from other sources shall be clearly defined. Work from other sources shall be properly referenced using an acknowledged referencing system.

The thesis shall be submitted in two bound volumes, signed by the candidate, and as an electronic file.

Supervisor   : Egil Pedersen, Department of Marine Technology, NTNU.

Co-advisor(s) : Dr Kensuke Kirimoto, Department of Engineering and Safety, UiT.

Start   : 01st January, 2012.

Deadline   : 10th June, 2012.

<div align="center">

Trondheim, 01st January 2012

Egil Pedersen

</div>

Preface

This master thesis is submitted in fulfillment of TMR 4925 Nautical Science Master Thesis which is a compulsory part of the international MSc program in Marine Technology, Nautical Science, NTNU.

The topic is selected by my personal preference which is the arctic maritime operation in terms of navigation systems. It was encouragement that I have written master project last year about safety for arctic operation, after finishing it I was thinking what I could do in this master thesis. Then I know that navigation bridge simulator is aiming to develop for high north operations but the icing module was obviously poor, here I found room to intervene my knowledge and contribution by making own computer code and analyse it.

I would like to thank my supervisor and mentor Prof. Egil Pedersen at Department of Marine Technology, Norwegian University of Science and Technology (NTNU). I would like to thank him for his supervision during this Master program. This program would not have been possible without his continuous guidance, suggestions and motivation, which are most appreciated.

I would also like to want thank Dr. Kensuke Kirimoto who assisted me with C++ source coding. My fellow students gave me motivation and encouragement every day, I appreciate their warm friendship.

Finally, my gratitude goes to my parents who support whole my two years master program in NTNU.

2012.06.10

Ryoji Kato

Modelling of Ship Superstructure Icing
- Application to Ice Bridge Simulators -

Abstract
Preface
Nomenclature and Abbreviation

Contents

Nomenclature

a	constant for spray flux [-]
A	surface area of cylinder [m^2]
b	constant for spray flux [-]
B	ship's breadth [m]
B_s	shape factor [-]
c	specific heat of fluid [J/kg·°C]
c_p	specific heat of dry air [J/kg·°C]
c_w	specific heat of water [J/kg·°C]
d	droplet diameter [mm]
D	characteristic length [m]
e	saturation vapour pressure [kPa]
e_a	saturation vapour pressure of air [kPa]
e_s	saturation vapour pressure of equivalent surface temperature [kPa]
E_c	collection efficiency [-]
GM	the metacentric height [m]
h	heat transfer coefficient [W/m^2·°C]
H_s	significant wave height [m]
k_f	thermal conductivity of the fluid [W/m·°C]
K	radius of gyration [m],
K_a	thermal conductivity of air [W/m·°C]
K_c	coefficient for heat transfer coefficient [$Wm^{-2.6}s^{0.8}$°C^{-1}]
l_f	latent heat of freezing [J/kg]
l_v	latent heat of vaporization [J/kg]
m	body mass [kg]
M_i	icing intensity [kg/m^2s]
M_w	total water flux [kg/m^2s]
n	freeing fraction [-]
Nu	Nusselt number [-]

N_i	icing intensity per hour [mm/h]
p	atmospheric air pressure [kPa]
Pr	Prandtl number [-]
q_a	heat conducted to or from the icing surface through the underlying structure [W/m^2]
q_c	heat transfer by convection to the surrounding air [W/m^2]
q_e	heat transfer by evaporation to the surrounding air [W/m^2]
q_f	latent heat of freezing a certain fraction of the impinging water [W/m^2]
q_w	heating (or cooling) of impinging water to the equilibrium surface temperature[W/m^2]
Q	total heat [J]
Re	Reynolds number [-]
S	sea water salinity [ppt]
Sc	Schumidt number
U, U_0	surface wind speed [m/s]
U_{10}	mean wind speed at 10 m elevation [m/s]
V	ship speed [m/s]
w	liquid water content [kg/m^3]
w_i	weight of ice around pipe [kg/m]
z	elevation from MWL [m]
α_r	relative angle of spray flux [degree]
β	constant defined by wind force [-]
ε	ratio of molecular weight of water vapour and dry air [-]
ζ	parameter of collection efficiency [-]
θ	temperature [°C]
θ_a	air temperature [°C]
θ_d	droplet temperature immediately prior to impingement [°C]
θ_f	freezing temperature of water [°C]
θ_s	equilibrium surface temperature [°C]
ρ_{ice}	density of ice [kg/m^3]

Abbreviation

DNV	Det Norske Veritas
JCG	Japan Coast Guard
LPG	Liquefied Petroleum Gas
LWC	Liquid Water Content
MWL	Mean Water Level
NSR	Northern Sea Route
VLCC	Very Large Crude oil Carrier

Chapter 1 Introduction

1.1 Background and Motivation

There have been increasing maritime activities in the high north region. For instance new oil and gas fields were discovered or expect to be discovered in the Norwegian Sea and Barents Sea. The discovery of the Skrugard oil field has started productions in April 2011. Volumes are estimated to be around 250 million barrels of recoverable oil equivalents, with a considerable upside potential. There are several prospects in the near vicinity, which is not only oil and gas industries; Northern Sea Route (NSR) is watched by ship operational company whose ships navigate between Europe and Far East for the benefits of reducing fuel consumption. Japanese ship owner/operator Sanko Steamship Company have opened services to transport bulk through NSR, they had introduced two DNV Ice Class 1-A ships which was to be owned by Danish ship owner afterward.

In the high north regions extreme weather conditions are assumed, historically Norwegian fisherman, seal and whale hunters have been struggling for this severe environment. One problem which must be considered during winter operation is icing. Fisherman has known for a long time how serious icing on fishing vessels may be because it reduces stability of ship and capsize in the worst case, accompanied with stability reduction due to free surface effect.

As the arctic operational demand increase, safety problems come up. Especially skilled maritime personal for ship navigation will be strong focus in order to maintain safety operation. When one operates on such a severe environmental condition special precautions should be provided including regulation and training prior to its commencement. Improved training programs of ship officers and pilots on a full-mission ice-breaker navigation simulator should be provided. Operational training would be done by using ice bridge navigation simulator. Kongsberg Maritime have introduced Ice Bridge Simulator POLARIS, whose additional ship icing module is not realistic and inaccurate. There are rooms of improvement regarding this ice module to which this thesis will contribute.

"Ship Superstructure Icing" or ice accretion will be observed when the vessel operating in the extreme weather conditions, i.e. very low temperature and strong wind conditions; generally it is on the high north region including great lake in North America, Baltic Sea, and high south regions. It causes a lot of harmful result. Ship Icing is also referred to as topside icing; because icing on the ship structure reduces the metacentric height which ending up with capsize in the worst case. Approximately 10 vessels are lost annually in northern latitude regions (Zakrzewski 1986). In Japan fishing boat that sank because of ship icing is reported as 23, moreover 360 persons missed (11 persons dead of cold found on the rubber boat) only two of them are rescued, report by the 1st Regional Coast Guard Headquarter of Japan in 1960' (Ono 1974). Icing on deck interferes with ship's missions and the accumulation of ice on antennas makes radio communications difficult and has a detrimental effect on radar systems (Thomas 1991).

Many researchers note that sea spray as the main reason of sea water flux rather than rain, drizzle, snow, and direct flooding on a ship deck or green water (Zakrzewski 1986, Tabata 1963, Thomas 1991). This is also contribution toward the maritime operations at the high north. That is why the study relating to the vessel icing is crucial part on the maritime safety.

Ship Superstructure Icing

Study Field

Computer Systems
Meteorology
Marine Hydrodynamic
   •Spray droplet behaviour
   •Wave prediction theory
Thermodynamics
   •Icing intensity

External Condition

Weather
   •Air temp.
   •Sea temp.
   •Relative wind force
   •Barometric pressure
   •Droplet diameter
Sea State
   •Wave height
   •Wave period

Ship Information

Displacement
Body Size
   •Length
   •Breadth
   •height
Draught Condition
   •Cargo
   •Ballast
Superstructures
   •House
   •Hand rail
   •Bulkhead
   •Life boat

Ice Bridge Simulator

Hard
   •Navigation bridge equipment
   •Display

Soft
   •Ship mathematical model
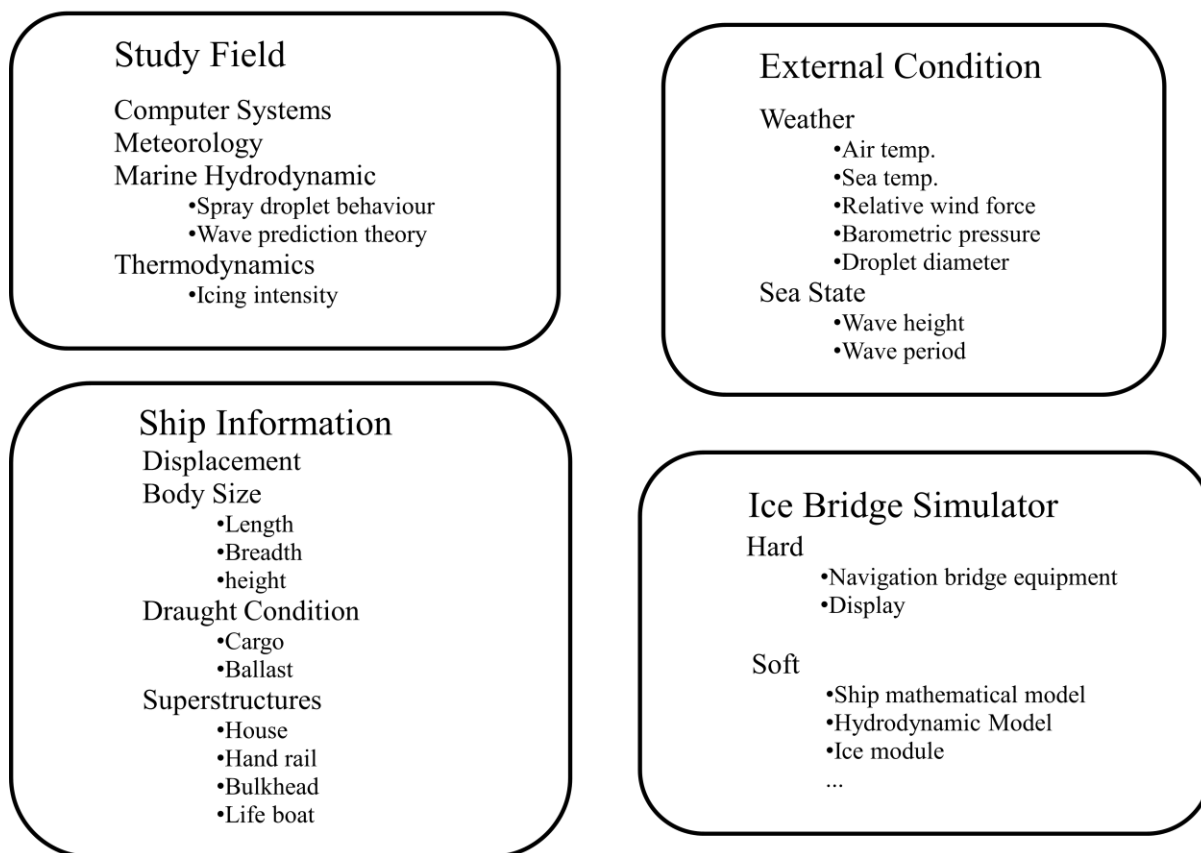   •Hydrodynamic Model
   •Ice module
   ...

Figure 1.1 Overview of the ship superstructure icing including different disciplines.

Free surface effect due to trapped water on the deck is additional threat. It is because of icing which compensates the opening between vertical hand rails and the bulwarks. Bulwark means a solid wall enclosing the perimeter of a weather or main deck for the protection of persons or objects on deck (Dictionary.com).

Due to increasing operational demand at the high north regions followed by needs of increasing number of sea training, ice bridge navigation simulator of Kongsberg Maritime was launched at University in Tromsø on winter 2011. From operational view point, it is essential that simulator training has a high degree of reality. But the newly (2011) installed ice module is not realistic and inaccurate. Thus more realistic model of ship superstructure icing shall be developed. Although icing model was introduced by Horjen (1983), Tabata (1963), Stallabrass (1980) and Zakrzewski (1986), those models have not been investigated yet with full scale measurement. Hence this thesis reviews the atmospheric icing on vessels aiming at incorporate an improved model to the ice bridge simulator for testing and evaluation purposes.

1.2 Previous Work

Ship icing has been recognized as a serious problem for a long time especially for small fishing boats cruising high north and has been discussed in the scientific literatures for more than one hundred years (Makkonen 1984). From 1960s theoretical sea spray models and computational methods to

calculate ice loads on a structure had been studied by several authors. In order to obtain computational parameters field test have been done by Tabata et al. (1963), Stallabrass (1967), Tabata (1969), and Stallabrass (1980). On the other hand icing mechanism or we could say thermodynamics processes have been studied by Horjen (1981) and Makkonen (1984), also Zakrzewski (1984) had developed sea spray configuration without considering thermodynamics. An algorithm of the ice accretion on structures has been numerically researched by Horjen (1983) and Zakrzewski (1988). In more recent years the numerical solutions had been further developed by several authors, for example Chung et al. (1995) had analyzed the distribution of ice accretion on mesh divided ship structure, although he assumes that ice accrete the ship's wall evenly which is not the case of real life, the paper shows us a blue print of numerical ice modelling. In recent years according to the increasing rigs used for oil exploration and drilling, sea spray icing on fixed offshore structures by the two dimensional analysis were studied (Jones et al. 2009).

Until now there are no icing model constructed that is able to be applied on ship navigation simulator and also free surface effect by trapped water on deck due to built ice between hand rails. Most recently Chung et al. (1995) has developed model for spraying of a stern trawler using data of 1:13.43 scale model by wind tunnel test. Although spraying model is based on laboratory test, rest of them, for instance freezing rate is based on thermodynamics/theoretical process.

Zakrzewski (1989) have studied two icing models, "the time-dependent Norwegian icing model" and "The University of Alberta ship spraying/icing model". In his paper algorithm of two model cases is explained with its mathematical model of icing. Both icing model will be tested using field data collected by Zakrzewski and Blackmore on the *M/T Zandberg* in the North Atlantic Ocean. The conclusion is that two models could not predict ship icing rate on *M/T Zandberg*.

Zakrzewski (1991) has studied ice growth rates and ice loads on the front parts of superstructure (i.e. bulkhead) for a medium-sized fishing trawler, based on software CONCICE that has been developed by University of Alberta. The model has been extended by superimposing a 7 x 13 numerical grid network on the bulkhead (grid cell size 0.5 x 0.5 m). The liquid water content (LWC) in the spray cloud is calculated by using the equation of Zakrzewski (1987). From computational result, the closer interval of bulkhead positioned at the ship's bow, the larger ice load estimated. In his context he suggested that ice allowance permitted by the government organization is needed for ship safety (e.g. 15 kg/m^2).

Distribution of spray droplet in the near-water layer shall be studied for developing computation of LWC. The vertical distributions of water content (LWC) [kg/m^3] in the lower layer of the atmosphere above the sea under moderate and strong winds can be estimated by exponential functions (Preobrazhenskii 1973).

Theory of ice accretion in Chapter 2 is mainly based on above literatures.

1.3 Present Work

1.3.1 Scope of Work

Scope of this thesis is to apply the developed computational method of ice loads to include free-surface effect due to trapped water on deck for its installation to ice bridge simulators. Modeling new algorithm of ice accretion which shall be integrated into ice bridge simulators would be constructed. Sufficient amount of literature work is necessary to figure out empirical formulas on a first stage of this research. This thesis shall not include any experimental test like tank test, wind tunnel test, field test, etc. because of limited working period of one semester, but it is quite clear that we can obtain sufficient amount of field data from past work that is also why relating tests shall be excluded on this paper.

1.3.2 Contribution

Until now a lot of studies have been done which relate to ship icing, but none of them could integrate the suggested model into ship navigation simulators. At the same time no navigation simulator can simulate ship icing phenomena with high reality although ice bridge simulator POLARIS by Kongsberg Maritime had installed with low reality of ice module in winter of 2011. From safety operational view point high reality module should be developed on the system. Since we consider the durational period as to be short for training scenarios on navigation simulator, sudden capsizing induced by free-surface effect should be included on the developed algorithm.

1.3.3 Organization of the Thesis

In chapter 2 the mathematical model or theory of ship icing are discussed from empirical relation. Firstly the reason of ship icing is introduced, and how to calculate LWC and freezing fraction are discussed. This part is mostly based on literatures. Those findings are used for computer program of ship icing.

In chapter 3 the theory of ship stability is discussed for the development of ice model in terms of stability change. Relation between centre of gravity and metacentre is discussed because it reveals stability criteria. This part is mainly by literature study from book "Ship Stability" Barrass and Derrett 2006.

In chapter 4 the concept of the ice model is discussed with its theologies. How to simplify ship structure, the way to obtain dynamic model, how to deal with free surface problem, are discussed. In this chapter specific equations are not stated, over view of the model algorithm is discussed.

In chapter 5 flow chart of the source code is explained. In proposed model 300 tonnage size of coast guard vessel are analyzed and superstructures are simplified with body shape. Validation of the function that calculates ice load and GM had done by comparing the model with field research.

In chapter 6 investigation of the model is discussed by analyzing two case studies. It is not easy to validate ship icing; some assumptions have been made for the comparison purpose. This chapter decides the degree of model reliability for installing into bridge simulators.

Concluding remarks are given in Chapter 7 with recommendations.

Chapter 2 Ice Accretion on Geometrical Structures from Empirical Relation

2.1 Introduction

Under severe weather condition when water particles collies with ship's superstructure considerable amounts of ice may accumulate. When the air temperature goes down below -3 °C ice accretes on the deck structures, and if lower that -6 °C the icing rate increases, moreover icing happens even if air temperature is not much lower than -3 °C if Beaufort scale is more than 3 (Tabata 1969). Figure 2.2 shows icing severity with parameter as air temperature and relative wind speed, findings are:

 i) For ship's size of 350 to 450 tonnes, icing occur from wind speed of 6 to 8 [m/s], but such wind speed is little bit higher for 450 tonnes ship.

 ii) Ice accretion start even at the air temperature minus 2 °C.

 iii) The stronger wind and colder temperature, severe icing will be observed.

By the research of British Ship Building association, the icing intensity show most strong rate at minus 17 °C, after that icing rate decrease (Tabata 1963).

As mentioned on the former chapter, there are several icing factors:

 (a) Super-cooled fog (referred to as arctic frost smoke or black frost)

 (b) Freezing rain or drizzle

 (c) Rainy snow

 (d) Freezing sea spray

Above mentioned, rainy snow is easy to be blown away and also due to less density, not to be regarded as a main factor, and also not for supercooled fog (Tabata, et al. 1963). In these, freezing of sea spray is the major factor of icing. See Table 2.1, 80 % of ship icings are due to sea spray, in this table data of the Arctic Sea does not show that sea spray is the main reason, but this is because of less number of data which referred to "unknown". Hence in our study sea spray is considered to as a main factor of ship structure icing.

Figure 2.1 Sea splashing made by collision between ship's bow and encountered wave, those icing on rigging can be observed due to wave-generated sea spray. (From Canadian Coast Guard HP, http://www.ccg-gcc.gc.ca)

Table 2.1 Statistical investigation of the icing causes of icing by different author. Mostly it is depend on sea spray. Data are collected from different author stated in "Reference" row.

| Region	Total number of observations	Cause of icing (%)			Reference
		Sea Spray	Spray and fog or rain or snow	Other types	
All seas	400	89.0	7.0	4.0	Shehtman (1968)
North Pacific	3000	89.8	7.5	2.7	Aksjutin (1979)
Arctic	Unknown	50.0	41.0	9.0	Aksjutin (1979)
Gulf of St. Lawrence	100	81.0	2.0	17.0	Brown and Roebber (1985)
Scotian Shelf	536	94.2	3.0	2.8	Brown and Roebber (1985)
Grand Banks	100	97.0	2.0	1.0	Brown and Roebber (1985)
NE Newfoundland Shelf	233	95.9	1.4	2.8	Brown and Roebber (1985)
Labrador Sea and Davis Strait	72	86.9	11.1	1.7	Brown and Roebber (1985)
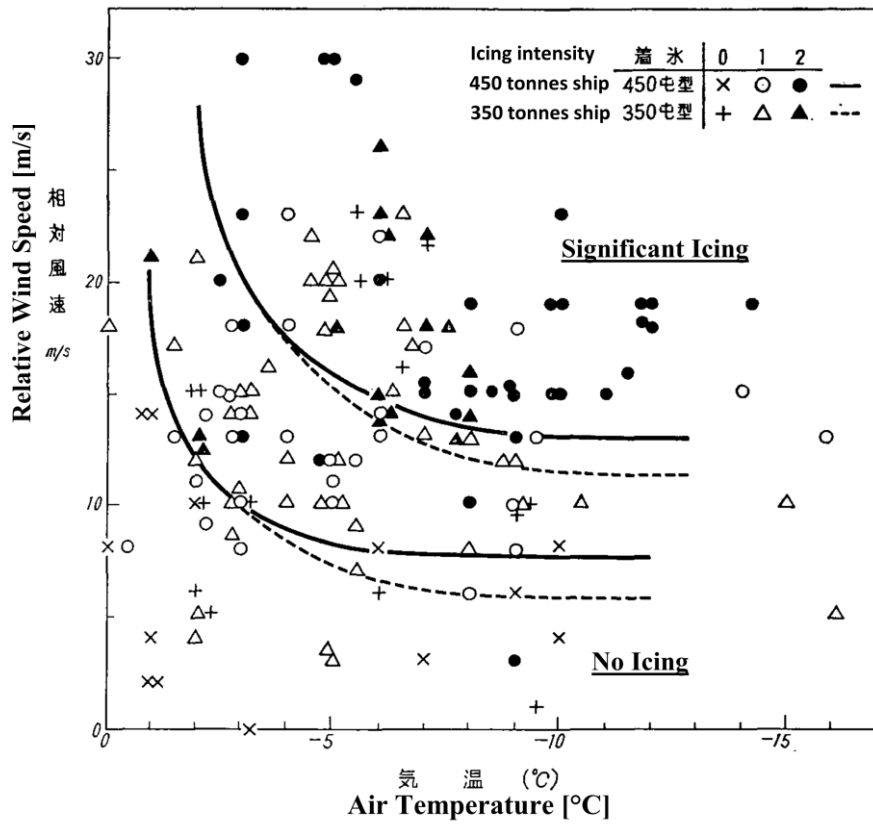
Figure 2.2 Icing severities as related to air temperature and wind speed. Icing intensity is defined by; 0 = no icing observed, 1 = small amount of ice is observed, 2 = strong icing is observed. (From Tabata 1969).

Table 2.2 Beaufort scale (Data source: National Oceanic and Atmospheric Administration)

Force	Speed (mph)	Speed (knots)	Description	Specifications
0	0-1	0-1	Calm	Sea like a mirror.
1	1-3	1-3	Light Air	Ripples with the appearance of scales are formed, but without foam crests.
2	4-7	4-6	Light Breeze	Small wavelets, still short, but more pronounced. Crests have a glassy appearance and do not break.
3	8-12	7-10	Gentle Breeze	Large wavelets. Crests ben gin to break. Foam of glassy appearance. Perhaps scattered white horses.
4	13-18	11-16	Moderate Breeze	Small waves, becoming larger; fairly frequent white horses.
5	19-24	17-21	Fresh Breeze	Moderate waves, taking a more pronounced long form; many white horses are formed.
6	25-31	22-27	Strong Breeze	Large waves begin to form; the white foam crests are more extensive everywhere.
7	32-38	28-33	Near Gale	Sea heaps up and white foam from breaking waves begins to be blown in streaks along the direction of the wind.
8	39-46	34-40	Gale	Moderately high waves of greater length; edges of crests begin to break into spindrift. The foam is blown in well-marked streaks along the direction of the wind.
9	47-54	41-47	Severe Gale	High waves. Dense streaks of foam along the direction of the wind. Crests of waves begin to topple, tumble and roll over. Spray may affect visibility
10	55-63	48-55	Storm	Very high waves with long overhanging crests. The resulting foam, in great patches, is blown in dense white streaks along the direction of the wind. On the whole the surface of the sea takes on a white appearance. The tumbling of the sea becomes heavy and shock-like. Visibility affected.
11	64-72	56-63	Violent Storm	Exceptionally high waves (small and medium-size ships might be for a time lost to view behind the waves). The sea is completely covered with long white patches of foam lying along the direction of the wind. Everywhere the edges of the wave crests are blown into froth. Visibility affected.
12	72-83	64-71	Hurricane	The air is filled with foam and spray. Sea completely white with driving spray; visibility very seriously affected.

2.2 Icing Process

2.2.1 Mechanism of the Ship Icing

The ship icing is quite complicated as a nature to study thoroughly because we need to gather several discipline of research: the droplet dynamics, the fluid dynamics in terms of spray trajectory and thermal dynamics at the same time, but it may be expressed in simplified way by using water content in unit area, relative wind speed or the speed that the contents are conveyed relative to obstacle and icing rate which shows that how many percentage of the liquid water content will freeze; i.e. our approach is the way such that if we could get to know those values the ice weight per unit area per unit time will be defined.
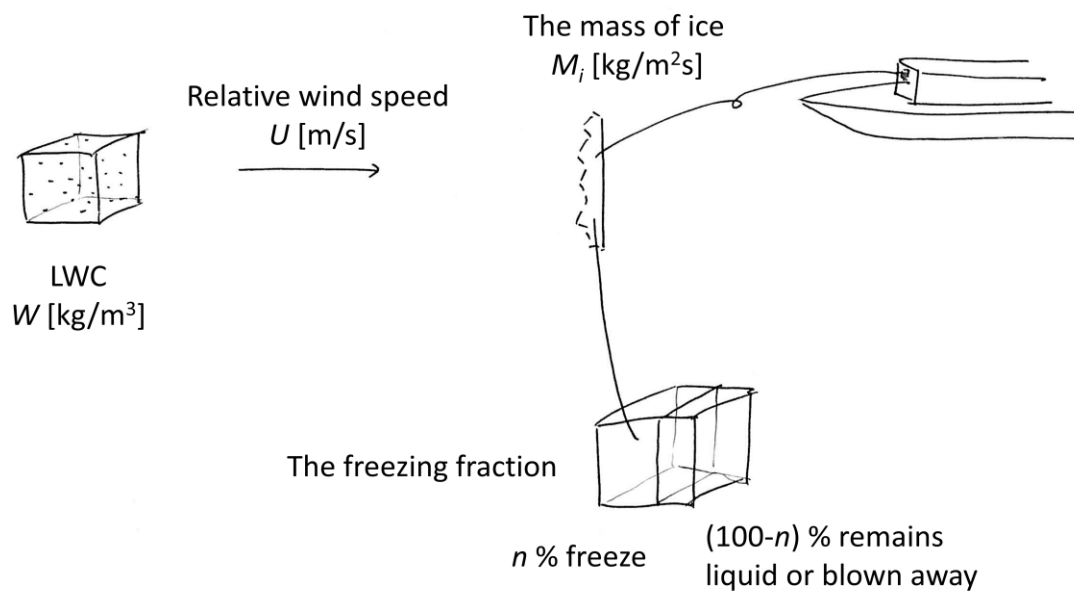
Figure 2.3 Mechanism of ice accretion process in simplified way. The mass of ice is expressed by LWC [kg/m³], relative wind speed U [m/s] and the freezing fraction n.

The amount of water flux of a cylinder and a flat plate to which unit area and unit time are expressed by the formula (Horjen 1983):

$$M_w = B_s E_c U w \qquad \text{[kg/m}^2\text{s]} \qquad (2.1)$$

where M_w = the amount of water flux [kg/m²s]

B_s = the shape coefficient [-] ($2/\pi$ for cylinder and 1 for plate)

E_c = the collection efficiency [-]

U = wind speed relative to object [m/s]

w = liquid water content [kg/m³]

The mass of ice forming on the obstacle (i.e. the amount of ice accumulates on the objected surface) is also expressed by the formula (Horjen 1983):

$$M_i = nM_w = nBE_cUw \qquad [\text{kg/m}^2\text{s}] \qquad\qquad (2.2)$$

where   n = the icing fraction [-]

All the diameters of the droplet are assumed to be equal in this expression.

In the next sub-chapter liquid water content are expressed.

2.2.2 Liquid Water Content

Liquid Water Content (LWC) is the measure of the mass of the water in a cloud in a specified amount of dry air. Here we divide the methods into two ways, (i) wind-generated and (ii) wave-generated spray, former one is the LWC made by wind and wave crest interaction and latter one is made by wave and ship interaction.

(i) Liquid Water Content for wind-generated spray
1. Kachurin et al. 1974:

The LWC of spray cloud is equally difficult to quantify in any unique way; however, Kachurin et al. 1974 suggests that wave height is the chief factor governing this parameter. As with droplet size, it may be assumed that the water content is also a function of the size, lines and speed of the vessel, and also a function of height above the sea surface. Kachurin et al. proposes that for the sailing speed of 6-8 knots and heading of 0 ±40°, a proportional relationship be assumed:

$$w = 10^{-3} H_s \; [\text{kg/m}^3] \qquad\qquad (2.3)$$

But in the icing model developed by Stallabrass 1980, it was found that LWC one sixth of that given by expression above result in a significant improvement in correlation with observed result. As a result, the expression for LWC

$$w = 1.7 \cdot 10^{-4} H_s \; [\text{kg/m}^3] \qquad\qquad (2.4)$$

has been adopted by Stallabrass 1980.

This expression is most simple but useful for modelling since this is not depend on object height, i.e. not like expression below. But disadvantage is that the ice formation will be same in terms of height which is not realistic, if the ship is tall this is not applicable.

2. Preobrazhenskii 1973:

The LWC is expressed as a formula;

$$w(z) = w_0 \exp\left[-\beta\left(z - \frac{H_s}{2}\right)\right] \qquad [\text{kg/m}^3] \qquad\qquad (2.5)$$

where H_s = significant wave height [m]

         z = object height above MWL [m]

w_0 and β is constant defined by the strength of wind,

i.e. $w_0 = 10^{-7}$ [kg/m^3] and $\beta = 0.35$ for moderate winds (U$_{10}$ = 7-12 m/s) and,

$w_0 = 10^{-5}$ [kg/m^3] and $\beta = 1.0$ for strong winds or near gale (U$_{10}$ = 15-25 m/s).

Actually the this expression is based on experiment that is shown in Figure 2.4 as a vertical distribution of spray water contents, that is why regression line is represented as to eq. (2.5). Alternatively Figure 2.5 shows LWC as a function of relative wind speed.
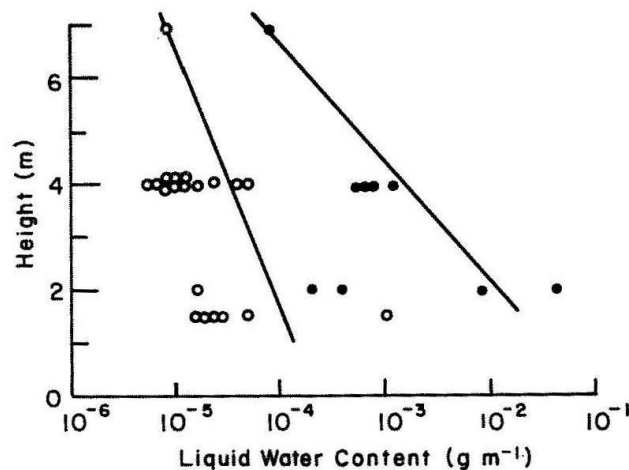
Figure 2.4 Liquid water content in the wind-generated spray as a function of the height above MWL (From Preobrazhenskii 1973 after Makkonen 1984). In this Figure eq. (2.5) is expressed by two linear lines.
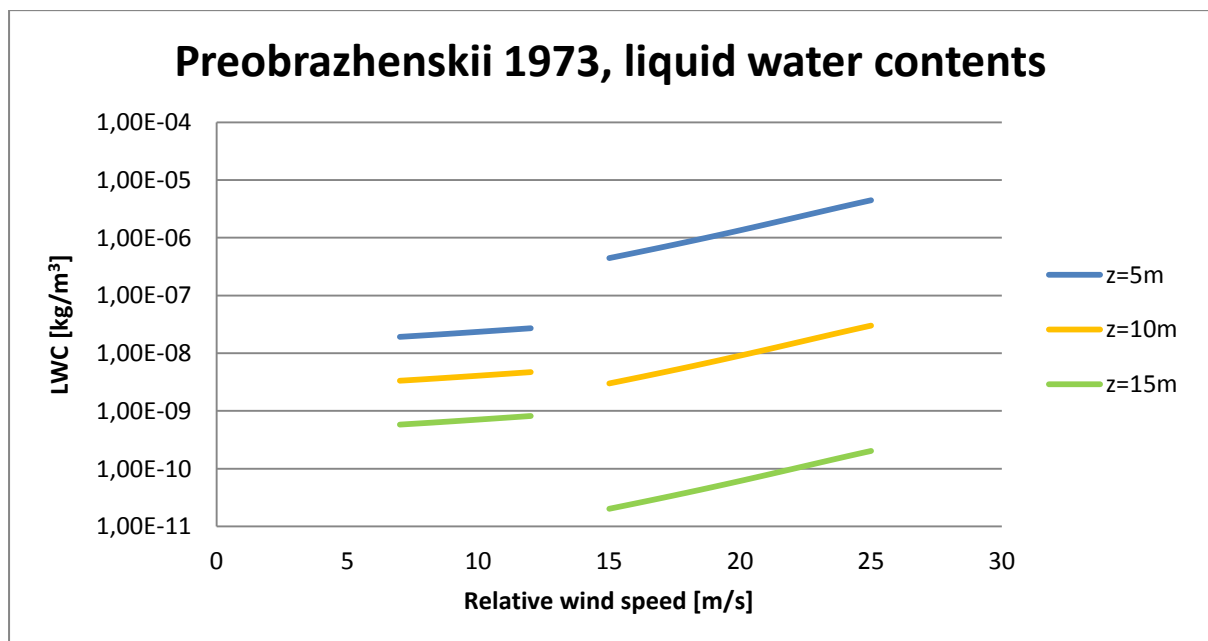
Figure 2.5 LWC as a function of relative wind speed. Note y-axis is expressed by logarithmic scale.

3. Horjen 1983:

In this expression LWC will decrease as z object height increase by second power of it, where mean wind speed at 10 meter height is used:

$$w(z) = 6.3185 \cdot 10^{-5} \cdot A(U_{10}) \frac{H}{z^2} \qquad \text{[kg/m}^3\text{]} \qquad (2.6)$$

where $A(U_{10})$ is a polynomial of the third degree in U:

$$A(U_{10}) = 0.01864 U_{10}{}^3 - 0.7943 U_{10}{}^2 + 11.3119 U_{10} - 53.5173 \quad \text{[m}^{-2}\text{]} \qquad (2.7)$$

4. Horjen and Vefsnmo 1984:

Here ration between wind speed at MWL and 10 meter height is used, decreasing exponentially;

$$w(z) = w_0 \left(\frac{U_{10}}{U_0} \right)^{3.8} \exp\left(\frac{H}{2} - z \right) \qquad \text{[kg/m}^3\text{]} \qquad (2.8)$$

(ii) Liquid Water Content for wave-generated spray
Horjen1983 proposed a guess for the wave-generated LWC:

$$w = \frac{1}{4} M_0' \frac{H^2}{z^2} = 2.5 \cdot 10^{-4} \frac{H^3}{z^2} \qquad \text{[kg/m}^3\text{]} \qquad (2.9)$$

$$w = M_0' \exp\left[-\beta \left(z - \frac{H}{2} \right) \right] \qquad \text{[kg/m}^3\text{]} \qquad (2.10)$$

where M_0 is defined by Kachurin et.al., 1974:

$$M_0' = 10^{-3} H_s \qquad \text{[kg/m}^3\text{]} \qquad (2.11)$$

Note that this formula is valid higher than the wave crest height, i.e. at z = H/2 (Horjen, 1983). And β is defined on the former section.

Horjen and Carstens 1989 has suggested theoretical formula to obtain the mean horizontal impact-generated spray flux, which means that mass flux per unit area:

$$G(z) = a \left(\rho_w g \frac{H_s}{U^2} \right) \left(\frac{K}{4\pi} \sqrt{gH_s} + V \cos\alpha_r \right) \left(\frac{2z}{H_s} - 1 \right)^b \quad \text{[kg/m}^2\text{s]} \qquad (2.12)$$

where   K = 12.077 [-]

              V = Ship speed [m/s]

              α_r = relative angle of spray flux [degree]

              a = 2.3489·10^{-6} [-]

              b = -2.0907 [-]

Those parameter "a" and "b" is empirically obtained by spray flux experiments on "Endre Dyrøy" reported by Horjen et al. 1986. Note that on his test four spray collectors were placed at the front mast

(14 m from the bow) at elevations 1.10 m, 2.00 m, 3.60 m and 5.35 m above the base of the mast. The highest wind speed was 18 m/s which means that the contribution from wind-generated spray may be neglected compared to the wave-generated spray. When we use this formula we may assume that relative angle of spray flux α_r shall be equal to 0 for simplification, which means the relative wind always come from right ahead. (In proposed model wind direction/ship course is not considered, here is room to improved for more realistic computation, see future work)

2.2.3 Heat Balance and Freezing Fraction
From wind tunnel test (empirical solution)

If the super-cooled water droplet impinges on the obstacles, it cooled down to freeze, the portion that does actually freeze on impact is called the freezing fraction n, and remaining fraction (1-n) as a watery contents are run off or blown off the surface. (See Figure 2.3) Freezing fraction can be obtained by both theoretical and empirical methods. Horjen 1983 has solved such relations by studying heat balance of the objective surfaces. On the other hand Stallabrass 1980 have been found out empirical relations by using wind tunnel test and demonstrated the effects of air temperature and cylinder size on the resulting ice formations. Firstly empirical approach is discussed in this sub chapter.

The icing tests were conducted in a closed circuit, refrigerated icing wind tunnel (Figure 2.6), in which the air is continuously recirculated by an electric fan demonstrate the effect of air temperature and cylinder diameter on the percentage of spray that freezes on the cylinder. Those test have been executed at National Research Council of Canada, although this data is taken in more than 40 years ago, since the reliability is quite high we adopt the test result into our analysis. The icing condition is produced by an array of water spray nozzles. Five cylinders, 3.8 [cm], 7.6 [cm], 15.2 [cm], 30.5 [cm] and 45.7 [cm] in diameter were used for the tests. Tests were exercised on each cylinder in both a horizontal and vertical orientation. The 3.8 [cm] cylinder was made of steel tubing 1.60 [m] long, and was mounted through flanged bushings in the tunnel walls. Other cylinders is 0.91 [m] long supported by 3.8 [cm] tube.

Wind speed was set at 43 kt (22.1 m/s) corresponding to a wind force of 9 on Beaufort Scale, air temperature is -14 °C and -7 °C. The water spray was set to give a water concentration in the air of 3.2 g/m^3 and droplet diameter is 0.2 mm. Representative drawing is shown in Figure 2.6, gravitational force act to deform the shape to as asymmetry, we can find that wind ward side (right side) has much ice apparently. Freezing fraction was calculated by weighing at the end of each 1-hour run, from formula from equation (2.2):

$$n = \frac{M_i}{AUw}$$

(2.13)

where   A = surface area of the cylinder [m^2].

Note the shape coefficient B_s is not considered in this case. The ice deposits were weighed at the end of each one hour run and the one hour icing efficiency (icing rate) determined. In spite of the difference in the shape of the ice accretions on horizontal and vertical cylinders (as a result of gravity affecting the run-off), no significant difference in icing efficiency was apparent (Stallabrass 1980).
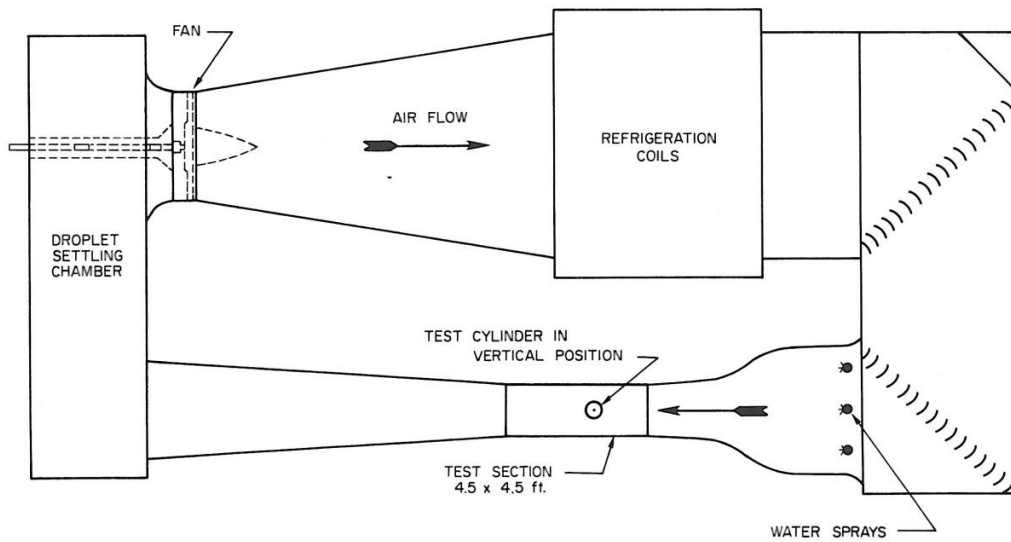
Figure 2.6 plane view of wind tunnel, (Stallabrass 1967) Capable of speeds up to 180 mph, and a temperature range of about -30 °C to room temperature. The air is continuously recirculated by a 1,000-hp electric fan. The icing condition is produced by an array of water spray nozzles.
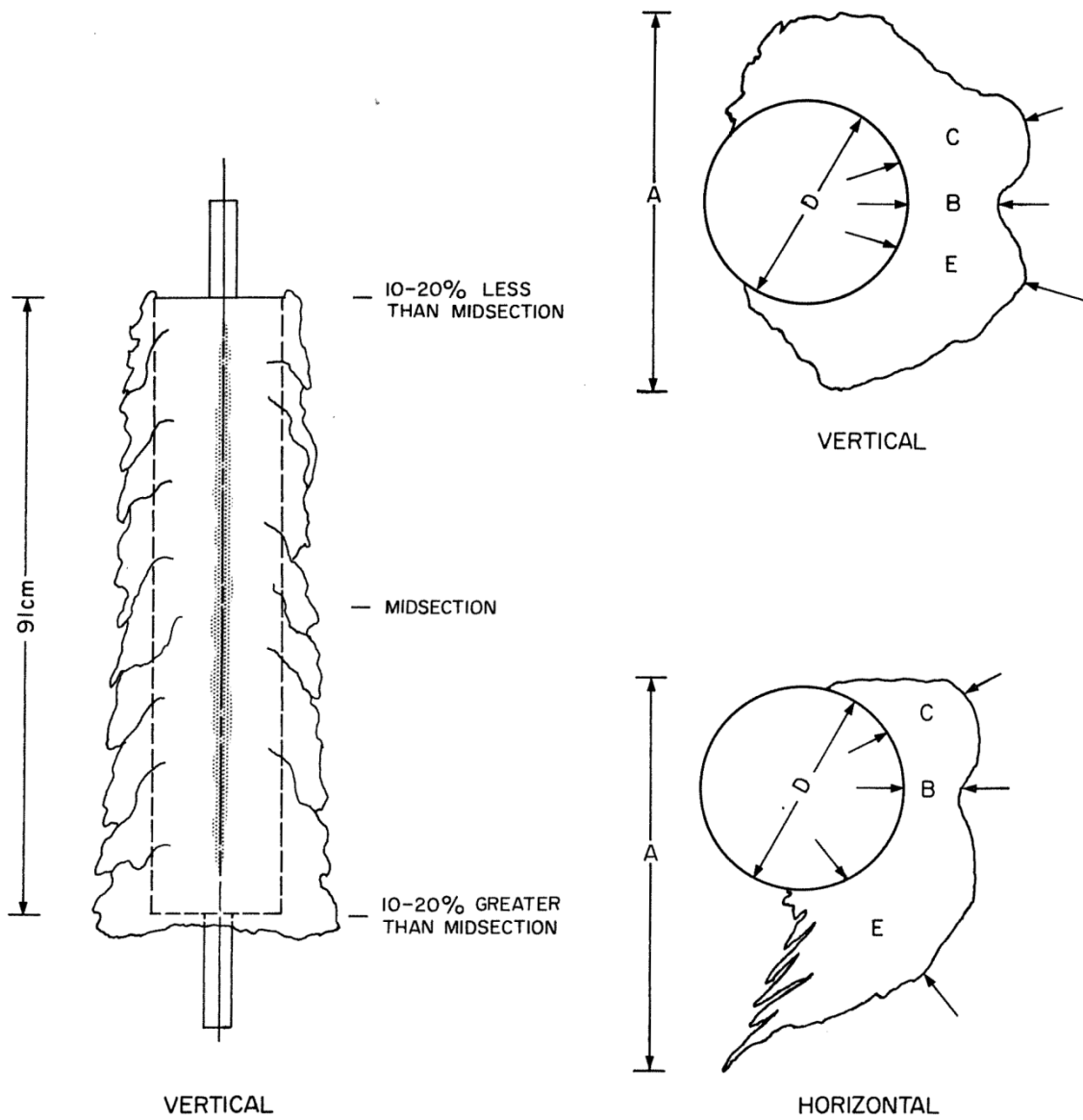
Figure 2.6 Dimensions of ice accretion by wind tunnel test, wind speed is 43 kt (22.1 m/s), droplet diameter is 0.2 mm, and water concentration in the air is 3.2 g/m³. Gravity contributes shape of ice to make it asymmetrical shape. (From Stallabrass 1980) The dimension A will be our main target for modelling (right below).
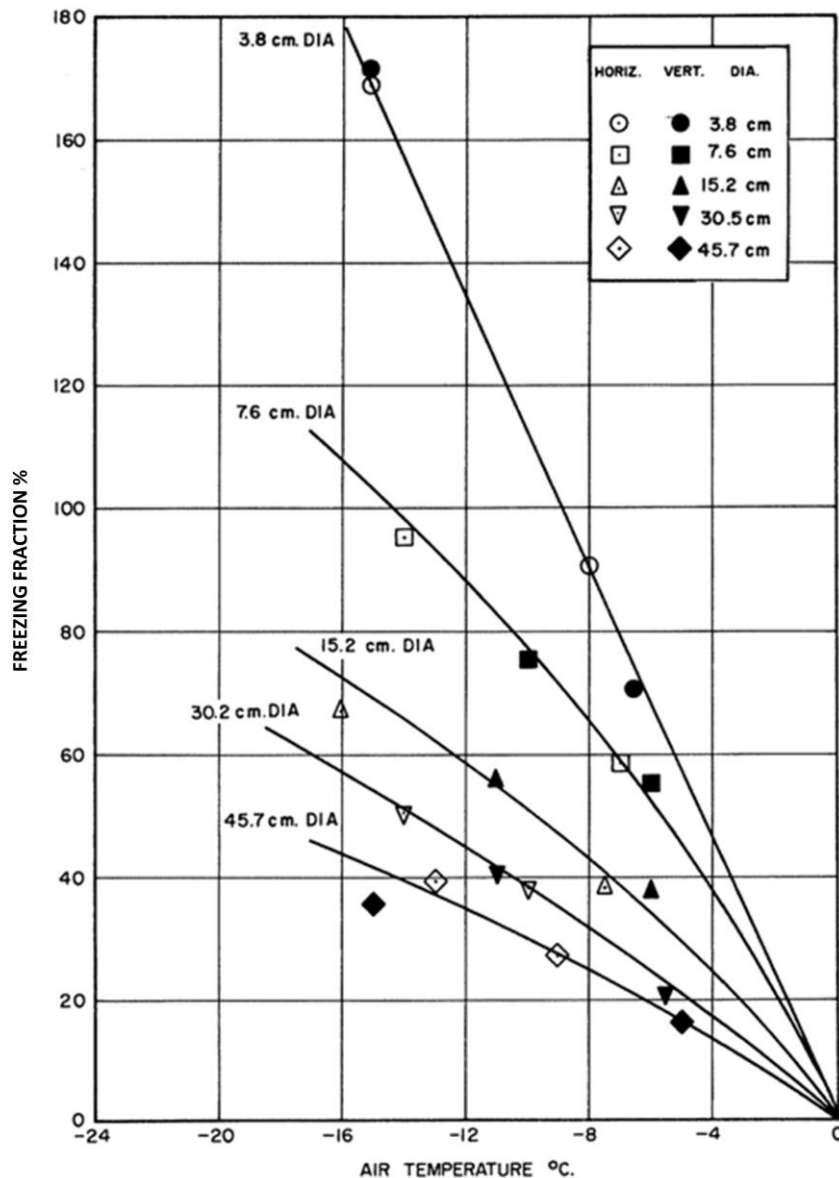
Figure 2.7 Effect of temperature on freezing fraction. This data is based on 21 times run. The relation shows linear/curve linear with air temperature and freezing fraction. (Picture source: Stallabrass 1980)

From typical findings from this test are:

- The dependence of the freezing fraction on the cylinder diameter and on the air temperature was demonstrated in Figure 2.7; the freezing fraction being shown to increase according to decreasing diameter and decreasing temperature.

- Freezing fraction does change with cylinder geometry (vertical or horizontal) if wind attack angle is normal to the object.

- Freezing fraction shall be considered that it has linear/curve linear relation with surrounding air temperature for all cylinder diameters.

16

In this test we should note the fact that the sea temperature is not considered. Also this relation is useful only when relative wind speed is 43 kt, which means there are difficulty to apply this model for whole structure of the ship with complicated shapes, also this test does not show data for the icing even for plates.

We could extract simple linear equation as a function of air temperature for computational purpose of ice accretion.

Depending on cylinder diameter:

$n_1 = -11.1\theta$ for diameter 3.8 [cm]

$n_2 = -7.5\theta$ for diameter 7.6 [cm]

$n_3 = -5.0\theta$ for diameter 15.2 [cm]

$n_4 = -3.8\theta$ for diameter 30.2 [cm]

$n_5 = -2.8\theta$ for diameter 45.7 [cm]

Although above relation is valid under restricted environmental conditions, i.e. wind speed U = 43 [kt], drop let diameter d = 0.2 [mm] and LWC w = 3.2 [g/m^3], these result help us to make blue print of ice accretion.

In this section empirical expression is delivered and analyzed. In the next section theoretical method is discussed.

From the thermo dynamics (Theoretical method)

The icing rate can be found from the thermodynamic process. Taking only the primary heat transfer processes acting at the icing surface into consideration, and assuming that the ice formation is continuous steady-state process, an equilibrium heat balance at the icing surface may be formulated as (Stallabrass 1980):

$$q_f + q_w + q_c + q_e + q_a = 0$$

(2.14)

where q_f : latent heat of freezing a certain fraction of the impinging water [W/m^2]

         q_w : heating (or cooling) of impinging water to the equilibrium surface temperature [W/m^2]

         q_c : heat transfer by convection to the surrounding air [W/m^2]

         q_e : heat transfer by evaporation to the surrounding air [W/m^2]

         q_a : heat conducted to or from the icing surface through the underlying structure [W/m^2]

Here we look into these heat coefficients respectively.

The latent heat term: q_f

Horjen (1983) suggested that the icing intensity M_i is expressed by following form by using icing fraction "*n*";

$$M_i = nM_w = nBE_cUw \qquad \text{[kg/m}^2\text{s]}$$

(2.15)

$$N_i = \frac{M_i}{\rho_{ice}} = 3.6 \cdot 10^6 \frac{nBE_cUw}{\rho_{ice}} \qquad \text{[mm/hour]}$$

(2.16)

The collection efficiency E expresses the degree to which the water drops in the air impinges on an object in their path, and is not deflected by the air blow around the object. The collection efficiency increases with relative velocity and with drop size, and decreases with the size of the object on which the drop impinges. Because the size of the water droplets involved in ship icing due to sea spray is large (>1 mm), they will be deflected little and the collection efficiency will be assumed to be 100%. This is also in order to make the computation procedure simple.

After all the heat released is:

$$q_f = l_f M_i \qquad \text{[W/m}^2\text{]}$$

(2.17)

where l_f is latent heat of freezing. (= $3.33 \cdot 10^5$ [J/kg])

Hence this term is expressed by wind speed, wave height and freezing fraction:

$$q_f = q_f(U, H_s, n) \qquad \text{[W/m}^2\text{]}$$

(2.18)

Heating of the impinging water to the equilibrium surface temperature: q_w

The heat given to the impinging water is expressed by

$$Q = cm\Delta\theta \qquad \text{[J]}$$

(2.19)

where   Q = total heat [J]

m = body mass [kg]

c = specific heat of fluid [J/kgK]

$\Delta\theta$ = temperature change [K]

then we can write the heating of impinging water to equilibrium surface temperature as:

$$q_w = M_w c_w (\theta_d - \theta_s) \qquad \text{[W/m}^2\text{]}$$

(2.20)

where c_w = specific heat of water (= 4000 [J/kg·°C])

θ_d = droplet temperature immediately prior to impingement [°C]

θ_s = equilibrium surface temperature [°C]

Tabata1963 has shown that the chlorinity and freezing temperature of the brine run-off is a function of the freezing fraction:

$$\theta_s = (1+n)\theta_f, \qquad 0 \le n < 1 \qquad\qquad [°C] \qquad\qquad (2.21)$$

Surface temperature can be said as equilibrium freezing temperature of water of the appropriate salinity. As ice forms at the surface, salt is rejected from ice crystal lattice so formed, and the water film on the surface of the ice manifests an enriched salt content. Since definite relationship exists between the salinity and the freezing temperature of the brine, which is expressed as:

$$\theta_f = -0.002 - 0.0524S - 6.00 \cdot 10^{-5} S^2 \qquad\qquad [°C] \qquad\qquad (2.22)$$

where S is salinity in parts per thousand.

The expression is for salinities between 0% and 40%.

As a result by using eq. (2.4) and (2.19) we obtain:

$$q_w = 1.7 \cdot 10^{-7} H_s c_w U (\theta_d - \theta_s) \qquad\qquad [W/m^2] \qquad\qquad (2.23)$$

Hence this term is expressed as a function of significant wave height, wind speed, droplet temperature and equilibrium surface temperature:

$$q_w = q_w(H_s, U, \theta_d, \theta_s) \qquad\qquad [W/m^2] \qquad\qquad (2.24)$$

Heat transfer by convection, (heat loss): q_c

Heat loss by convection with surrounding air is expressed in terms of a heat transfer coefficient, h, and the temperature difference between the surface and the surrounding air:

$$q_c = h(\theta_a - \theta_s) \qquad\qquad [W/m^2] \qquad\qquad (2.25)$$

where   h = the hear transfer coefficient [W/m²K].

The heat transfer coefficient is defined by body geometry, length and Reynolds number and Prandtl number. In determining an expression for the convective heat transfer coefficient, a certain amount of approximation is necessary since the shape and size of the icing surface is undefined.

For a flat plate in turbulent flow parallel to its surface (e.g. the deck of a vessel) an average heat transfer coefficient over a length L is given (Rohsenow et al. 1961) by:

$$h = 0.037 \frac{k_a}{L} \text{Pr}^{1/3} \text{Re}^{0.8} \qquad\qquad [W/m^2 \cdot °C] \qquad\qquad (2.26)$$

Only forced convective heat transfer will be considered. If a mean temperature of -5°C in the boundary layer above icing surface is assumed it may be shown that the "mean" heat transfer coefficient is given by:

$$h = K_c \frac{U^{0.8}}{D^{0.2}} \qquad\qquad [W/m^2 \cdot °C] \qquad\qquad (2.27)$$

where K_c = 5.17 [Wm$^{-2.6}$s$^{0.8}$°C^{-1}] for a cylinder (Stallabrass 1980) and K_c = 6.3279 for a flat plat (Horjen 1983) placed normal to the air stream (if the Reynolds number is larger than $4 \cdot 10^4$).

The convective heat term decrease as wind speed increase if the air temperature is lower than equilibrium surface temperature, in case of a cylinder, an example is shown in Figure 2.8.

Hence this term is as a function of relative wind speed, characteristic length, air temperature and equilibrium surface temperature:

$$q_w = q_w(U, D, \theta_a, \theta_s) \qquad \text{[W/m}^2\text{]} \qquad (2.28)$$
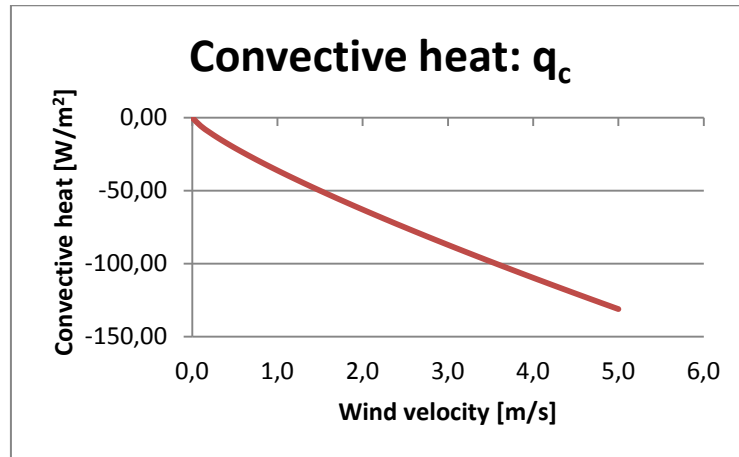
Figure 2.8 Example of convective heat term, air and equilibrium surface temperature is set as θ_a = -10°C, θ_s = -5°C.

Heat transfer by evaporation to the surrounding air: q_e

When the liquid evaporate to surrounding air the energy loses which is expressed as:

$$q_e = h \left(\frac{Pr}{Sc} \right)^{0.63} \frac{\varepsilon l_v}{p c_p} (e_a - e_s) \qquad \text{[W/m}^2\text{]} \qquad (2.29)$$

where Pr = Prandtl number (= 0.711)

   Sc = Schmidt number (= 0.595)

   ε = the ratio of molecular weights of water vapour and dry air (= 0.622)

   p = atmospheric air pressure

   l_v = latent heat of vaporization of water (= 2.5·10^6 [J/kg])

   c_p = specific heat of dry air (1.005·10^3 [J/kgK])

   θ_a, θ_s = saturation vapour pressure of moist air at temperature .

Using values above and rewrite equation:

$$q_e = 1731 \frac{h}{p} (e_a - e_s) \qquad \text{[W/m}^2\text{]} \qquad (2.30)$$

If we use h = 5.17V$^{0.8}$ [W/m^{2}K], and assuming p = 100 [kPa] then:

$$q_e = 89.5(e_a - e_s)U^{0.8} \qquad \text{[W/m}^2\text{]} \qquad (2.31)$$

where the saturation vapour pressure e_a and e_s may be expressed in [kPa] as a function of temperature by forth polynomial as:

$$e = 1.9226 \cdot 10^{-7}\theta^4 + 2.4545 \cdot 10^{-5}\theta^3 + 1.4224 \cdot 10^{-3}\theta^2 + 0.044436\theta + 0.61094 \quad \text{[kPa]}$$
$$(2.32)$$
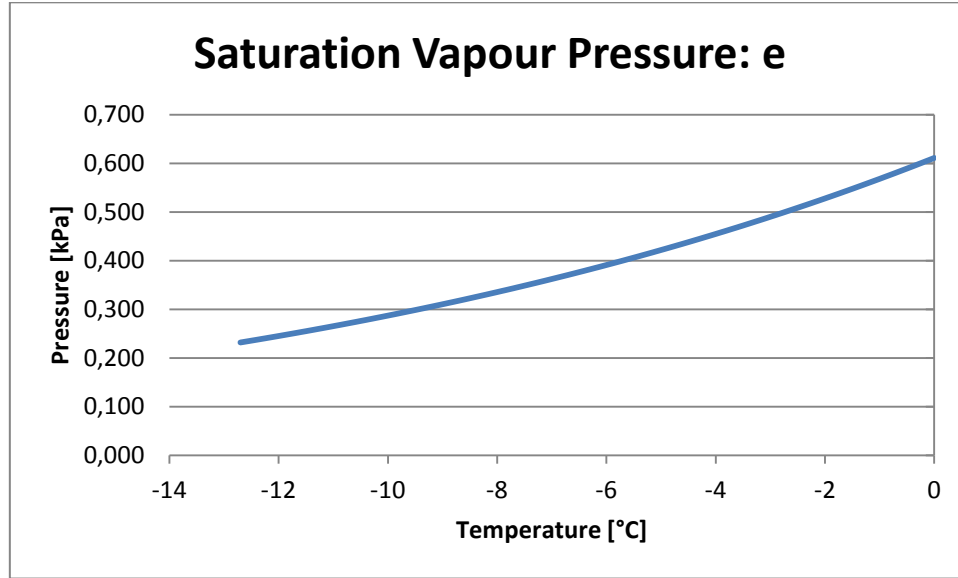
Figure 2.9 Saturation vapour pressure as a function of temperature. It decrease as the temperature decrease.

This means that q_e is a function of air/equilibrium temperature t_a t_s and wind speed U.

$$q_e = q_e(e_a, e_s, U) = q_e(\theta_a, \theta_s, U) \qquad \text{[W/m}^2\text{]} \qquad (2.33)$$

Total heat balance

From the formulas gotten from above derivation, we summaries by using eq. (2.14), (2.17), (2.23), (2.27) and (2.31):

$$l_f M_i + 0.68 H_s U(\theta_d - \theta_s) + 5.17 U^{0.8}(\theta_a - \theta_s) + 89.5(e_a - e_s)U^{0.8} = 0 \qquad (2.34)$$

here we used specific heat of water $c_w = 4000$ [J/kg·K], in case of cylinder and neglect contribution from characteristic length D since influence much small to the result. The latent heat released during freezing is $3.33 \cdot 10^5$ [J/kg]. So the above expression can be rewritten as:

$$M_i = 2.042 \cdot 10^{-6} H_s U(\theta_s - \theta_d) + 1.553 \cdot 10^{-5} U^{0.8}(\theta_s - \theta_a) + 2.688 \cdot 10^{-4}(e_s - e_a)U^{0.8}$$
$$\text{[m/s]} \quad (2.35)$$

by using ice density ($\rho_{ice} = 890$ kg/m^3) and express by [mm/hour] we get ice intensity, if as is more usual, using [mm/hour]:

$$N_i = \frac{M_i}{\rho_i} = 8.260 \cdot 10^{-3} H_s U(\theta_s - \theta_d) + 0.0628 U^{0.8}(\theta_s - \theta_a) + 1.087 U^{0.8}(e_s - e_a)$$
$$\text{[mm/hour]} \quad (2.36)$$

We should note that the saturation vapour pressure e is a function of temperature, equilibrium surface temperature θ_s is a function of salinity S and freezing fraction n. In order to get n and θ_d iteration procedure is needed.

Finally icing fraction is expressed by the ratio between total water flux and the amount of icing intensity:

$$n = \frac{M_i}{M_w} \qquad (2.37)$$

Iterative procedure to obtain freezing fraction n

In order to get freezing fraction n, simple iterative procedure is used. First n value is assumed to be zero, i.e. $\theta_f = \theta_s$. Subsequent iterations used the computed value of M_i to determine a new value of n, repeat this procedure until successive values of n differed by less than an arbitrary amount (e.g. 0.0001)

Iterative procedure to obtain droplet temperature θ_d

In order to get droplet temperature, first droplet temperature θ_d is set as same as sea water temperature θ_w, getting X_t.

$$X_t = 1 + 0.622 \frac{l_v}{p c_p} \frac{e_a - e_w}{\theta_a - \theta_w} \qquad (2.38)$$

Derive a new value of t_d by

$$t_d = t_a + (\theta_w - \theta_a) \exp\left[-\frac{6 Nu K_a}{\rho_w c_w d^2} X_t \tau \right] \qquad [°C] \qquad (2.39)$$

where   Nu = Nusselt number ($= \dfrac{hD}{k_f}$)

D = Characteristic length [m]

k_f = Thermal conductivity of the fluid (water) [W/m·°C] (= 0.58, by www.engineeringtoolboc.com)

K_a = conductivity of air [W/m·°C] (= 0.0243, by www.engineeringtoolboc.com)

This procedure is repeated until successive value of θ_d differed by less than an arbitrary amount (e.g. 0.0001 °C), where the duration of single sprays τ has measured 2.9 s by personal communication between Zakrzewski and Horjen (Horjen 1989).

Chapter 3 Transverse Stability

3.1 Stability Conditions

3.1.1 Notation for Chapter 3

The center of gravity G is the point through which the force of gravity is considered to act vertically downwards with a force equal to the weight of the body. The center of buoyancy B is that point through which the force of buoyancy is considered to act vertically upwards with a force equal to the mass of displaced water by submerged volume. The centre of buoyancy moves freely with regards to ship's motion and K means the centre point of bottom plate or "keel". See Figure 3.1(a).

(a)   (b)
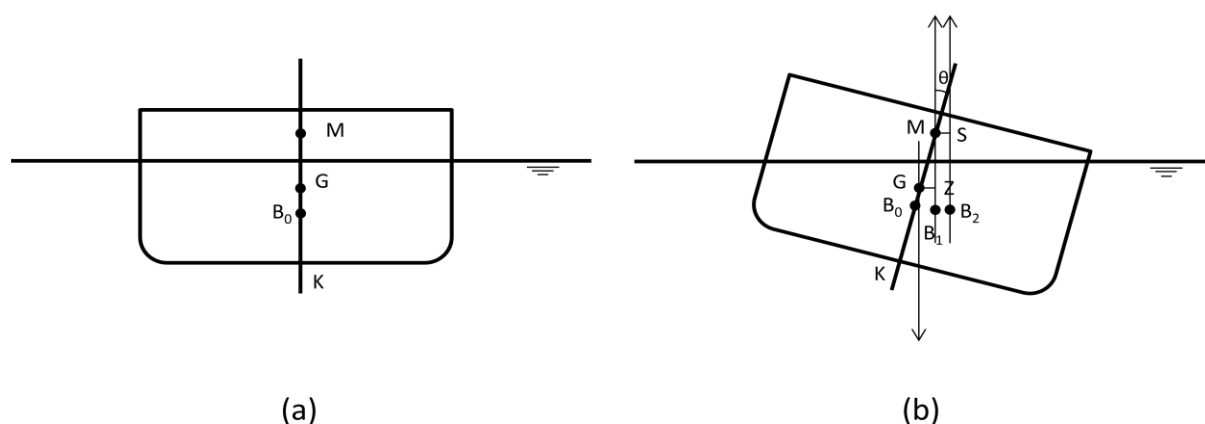
Figure 3.1 (a) Definition of the centre of buoyancy, gravity, keel and metacentre with its equilibrium condition. (b) The stable ship condition with small heel angle θ, linear relation between lever GZ and θ can be observed as shown in eq. 3.2. Note the centre of buoyancy B will move as the ship incline because of dependence of underwater ship's form.

3.1.2 The Metacentre including the Definition of Rest Stability Arm MS (θ)

If the ship is affected by some external forces like wind and wave the ship is heeling in small angle with the centre of gravity does not change since the distribution of ship's mass does not, the vertical through the new centre of buoyancy and initial center line intersect at a point called the metacentre, see Figure 3.1(b). The height of the initial metacentre above the keel depends upon a ship's underwater form.

Stable equilibrium

The ship return to the initial position if ship is in the stable equilibrium, in order to be in this condition the centre of gravity must below the metacentre and it is called the ship has positive GM as shown in Figure 3.1(b). The centre of buoyancy moves out and centre of gravity of submerged volume of displaced water, which vertical through metacentre. If the moments are taken about G there is a moment to return the ship to the initial position, that is referred to as the "Moment of Statical Stability" and is equal to the product of the weight force W and the length of the lever GZ; i.e.

$$\text{Moment of Statical Stability} = W \cdot GZ \tag{3.1}$$

The lever GZ is referred to as the "righting lever" and is the perpendicular distance between the centre of gravity and the vertical through the new centre of buoyancy B_1. GZ is if the angle of heel is small, or less that $5°$ the rest stability can be neglected.

$$GZ (\theta) = GM \sin\theta + MS (\theta) \qquad\qquad (3.2)$$

hence

$$\text{Moment of Static Stability} = W·GZ (\theta) \qquad\qquad (3.3)$$

Note since the metacentric height depends on ship's underwater form, GM increase as the heel angle will. S is the point of the vertical axis through M at any angle of heel. If the heel angle exceeds the value at which maximum GZ is observed GM start decreasing, when the angle of heel at which the righting lever returns to zero (GM = GZ = 0), the stability will be unstable and no more uplifting force will be expected (the angle of vanishing stability). These characteristics are well expressed by using the "GZ curve" which is identical not only by ships type/size but also ship's loading condition including accreted ice.

Unstable equilibrium

If the ship is unstable condition, the centre of gravity of the ship G positions above the metacentre, external force induced small angle of heel will make further inclination due to momentum with its negative GM, Figure 3.2(a), which stability is not secured in this case and so as to capsize.

Neutral equilibrium

If the centre of gravity is at the same point to the metacentre, the ship's static condition is neutral equilibrium as shown in Figure 3.2(b). The ship is affected by external force to make heel angle θ but no stabilizing or capsizing motion will be observed since two vectors have equilibrium on the same vertical line (Barrass and Derrett 2006).

(a)   (b)
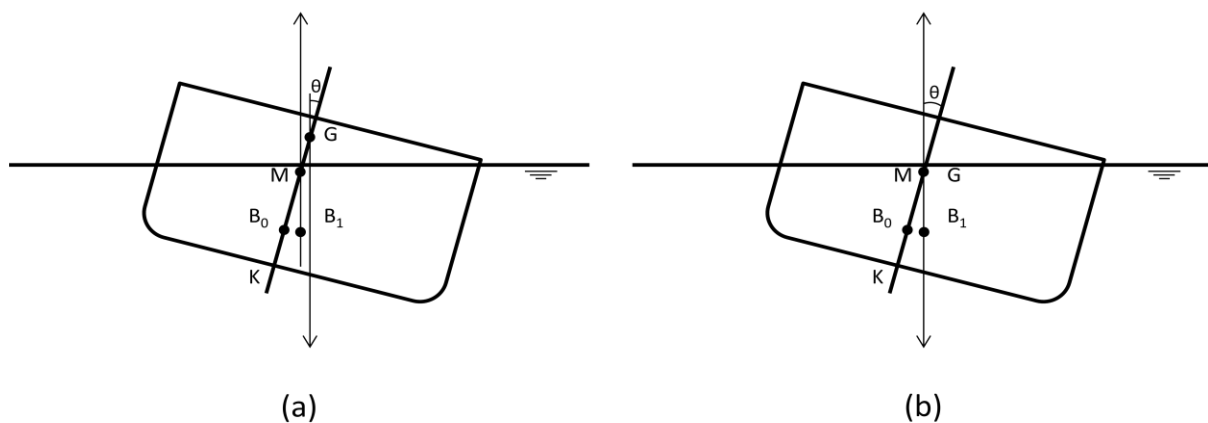
 Figure 3.2 (a) Unstable condition and (b) neutral condition. Note the relative position between centre of gravity and metacentre.

3.2 Free Surface Effect

If tank with filled liquid it can be considered as a fixed weight on ship geometry. But in case of the tank being not filled, those liquid make change of centre of gravity for and ship's centre of gravity. In our study when the hand rails on the brink of ship get icing making temporary ice wall, the water on

deck will make a same effect above deck initial centre of gravity is g. As shown in Figure 3.4, the ship heels and the liquid on deck flow to the low side such that its centre of gravity shifts from G to G_1, parallel to gg_1.

Hence

Moment of Statical Stability $= W \cdot G_1 Z_1$

$= W \cdot G_v Z_v$

$= W \cdot G_v M \sin\theta$ (3.4)

Even small GG_1 change, GG_v could be large and GM shorten as well. If the ship has small GM, thanks to free water reduction of GM induce large stability loss following with negative metacentric height.
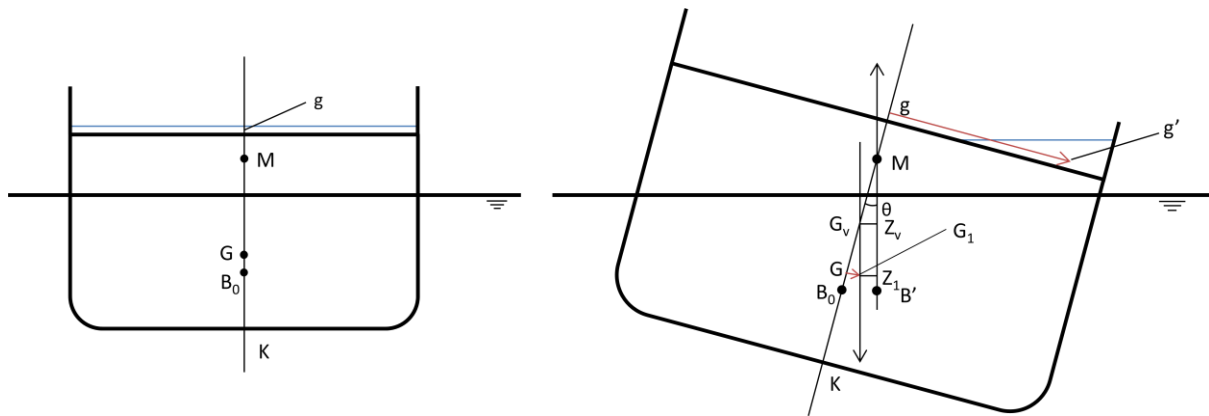
Figure 3.4 Image of free surface water on deck moving a centre of gravity right ward parallel to gg', resulting in reduced metacentric height as GM to G_vM, even if position G change small distance GG_v could be large.

3.3 Calculation of the Centre of Gravity

Centre of gravity changes due to ice load and expressed by using sum of momentum force, if we have ice load m the resultant KG height is expressed as,

$$KG' = \frac{KG \cdot M + Kg \cdot m}{M + m}$$
(3.5)

where   KG = Initial KG height [m]

KG' = resultant KG [m]

M = ship's displacement [kg]

Kg = distance between centre of gravity of the mass (ice) and keel [m]

m = mass (ice) weight [kg]

Chapter 4 Model Concept

4.1 Introduction

The model had been constructed aiming that to be installed to ice bridge simulators. Regarding the research direction overall picture of the blue print of the model is discussed, additionally new development unique to the model is also discussed. The general description has been done here, and a specific description will be done on chapter 5.

4.2 Concept of the Ice Model

An expected whole figure of the model shall be explained in this sub chapter. The blue print of the model, i.e. how the model is constructed, the final goal on the purpose of the model is further proposed with its functionality on the simulators. Needless to say, the low reality of the existing ice module of the simulators is our motivation.

Figure 4.1 Ice bridge simulator, picture of bridge console. picture source; http://www.uniteammarine.com

Concept of Ice Model
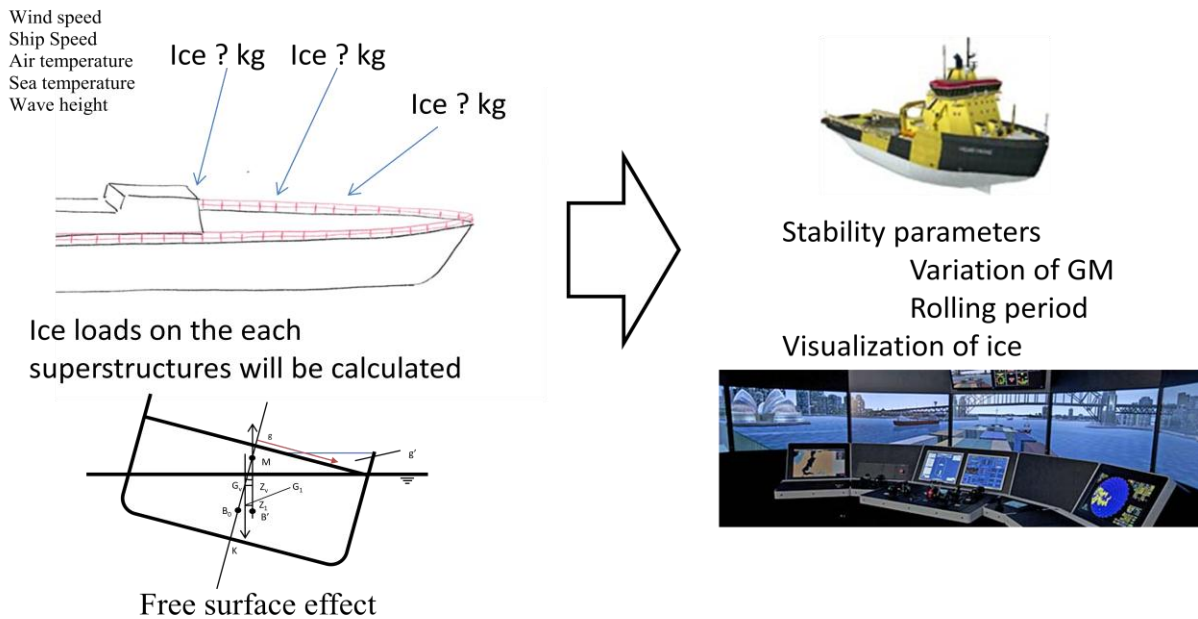
Figure 4.2 Model concept of ice module. Picture source of ship and simulator (right hand): Kongsberg Maritime http://www.km.kongsberg.com

First of all, the model shall essentially being able to be installed on all kind of bridge simulators regardless of the manufacturers. From this view point basic information of the simulator as a mother system should be studied including current development regarding the algorithm of icing module. Here we have asked for the information of ice module on the Kongsberg's ice bridge simulator POLARIS as a representative model of simulator system though, we could not obtain it on the technical aspect especially regarding the ice module because of a reason "company secret" which is expected too simple to calculate such a complicated phenomena of icing. That is why such information has been collected throughout internet and library all over Norway as much as possible both for qualitatively and quantitatively.

That is why a construction of a model with high reality has been a main target on our study. The input parameters should be detailed such as; both for air and sea temperature, wind speed, significant wave height, wind fetch, ship speed and cylinder diameter, etc. Additionally the simulation should be continuous during the duration of training which ranges of several hours. The calculation result is shown in a time domain that shall be done continuously or every second thought the training durations.

A basic calculation theory behind is set to an integration process by short cylinders and small plates which represent the superstructures above the upper/superstructure deck. Here we assume that those structures can be represented by gathering of cylinders and plates. Ship superstructures are simplified with high degree of reliability. Inclination of the plate is not calculated in proposed model though it should be considered with change of relative wind speed; we assume that relative wind speed is from right ahead.

Especially the reason of using cylinder as a representative element is that the opening between two parallel pipes can be a good object when simulating such sudden stability change due to trapped water

on deck, by the idea that ice building between two pipes (cylinders) make a temporary "wall" that blocks incoming water not to be able to escape out. There is another reason of using cylinders; sufficient empirical data could be collected from literatures of both full scale and cold temperature wind tunnel test (Stallabrass et al. 1967), from this view point we could say that cylindrical structure has a high reliability in order to represent super structures.
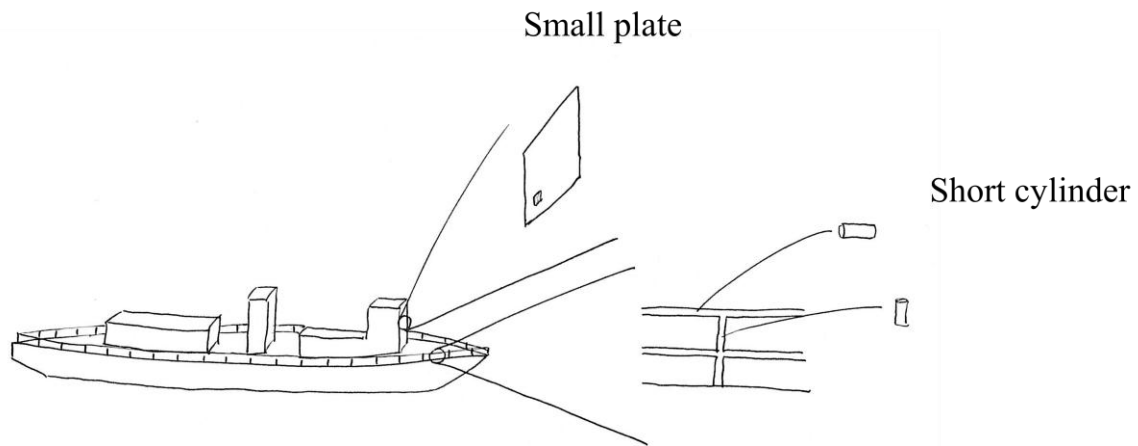
Figure 4.3 Model simplification concept, superstructure that have a possibility of icing, i.e. hand rail is assumed of gathering of cylinder. Most of the ship superstructures are assumed to be represented by the plates and the cylinders.

We have to say one more thing regarding this integration process. The subjected ship shape should be simplified for computational purpose, but not too simple on the point for the pursuit of realism. That is why the model shall not be simplified too much until that will be far from the reality.

Stability shall be calculated and evaluated by means of GM height (or simply GM). GM shall be calculated by hydro static table that is unique to each ship's hull shape respectively. GM can also be computed by rolling period, which is why navigator/trainee could notice its change of the rolling period that can be noticeable by the simulator display swinging the bridge view.

Final goal is the model installation to ice bridge simulator. Calculation speed shall be reduced as short as the requirement of the simulator system. If the calculation takes long period (e.g. one second), it means the program code cannot suit for the system.

In proposed model we assumed that winds are blown on to those cylinders and plates normal to it for simplification, but in real situation it changes with ship's course, wind speed, and also depend on ship's 6DOF and also depend on the geometry of the elements. In order to deal with this point, we should consider angle of those structure elements on the body fixed coordinate systems, assuming it moves with ship's 6DOF.

Finally after ice load and stability parameters are calculated those numbers should be notified to the ship navigators/simulator trainee. GM should be reflected to the system display in terms of scenery motion with ship rolling from which navigator can perceive the stability change.

4.3 Developed Features of the Ice Model

Free surface effect

As shown in "Chapter 1.2 Previous Work", Chung et al. (1995) have studied the sea spray as a main parameter of ship icing by theoretical solutions; i.e. spray trajectory equation. But "Water on deck and sudden stability reduction" had not been taken into account on their work. Such sudden stability reduction will happen if each opening of the hand rail of ship shall be compensated by accreted ice on the surrounding slender structure (hand rail), then green water poured into ship's deck cannot peep out and keep trapped on which behaves like a sudden emerging of an open top tank with its center of gravity being high, causing ship to capsize in worst occasion, this is also called "Free Surface Effect" that is of a problem in a liquid cargo ship whose cargo hold would not be fulfilled by liquid (i.e. crude oil, LPG etc.). As a result in our study, this problem is developed. (see Chapter 6, case studies)

Dynamic model

As a nature of simulator navigation training it should be a continuously being output in the duration of it. Those modules to be added on it must have a continuous system. From empirical research it is obvious that how thick does ice accretes on a decided diameter of cylinder per hour, which is static status. By summing up those numbers every hour/minutes and get a result as a form that is continuous.

Chapter 5 Computer Program

5.1 Introduction

In the former chapter model concept is described. Alternatively more detail shall be described in this chapter including model algorithm, flow chart, test run, simplified ship shape. Computer program has been done by using "Microsoft Visual C++ 2010 Express". 300 tonnage size coast guard vessels is picked up as an design object, with which the ship's superstructures are simplified, i.e. not consider detail but does not mean unrealistic, regarding this validation of the degree of simplification is discussed in chapter 6.

5.2 Flow Chart

5.2.1 Overview

The overview of the program structure is quite simple as shown in the Figure 5.1, we can find process of the icing module. A main function with two originally made function from empirical relation support the model. The computation process is; input environmental data such as wind speed, wave height, and air temperature etc. And read structure file of the object ship, i.e. x-, y- and z- coordinate of the subjected element, cylinder diameter, plate area, etc. Specific ice load calculation will be done on two function called "Ice_cylinder" and "Ice_plate", which is constructed from empirical formulation discussed in chapter 2. As stated on the next subsection, superstructures are assumed that gather cylinder and plate on deck and function is selected according to geometry. Finally the ice load and following metacentric height from keel (KM) is calculated by summing up all the ice load for each structure elements based on eq. 3.5. Resultant file is written at final part. The resultant file is composed of those coordinate information and ice load both for each element and total ship ice load following to GM change. See also Appendix E.
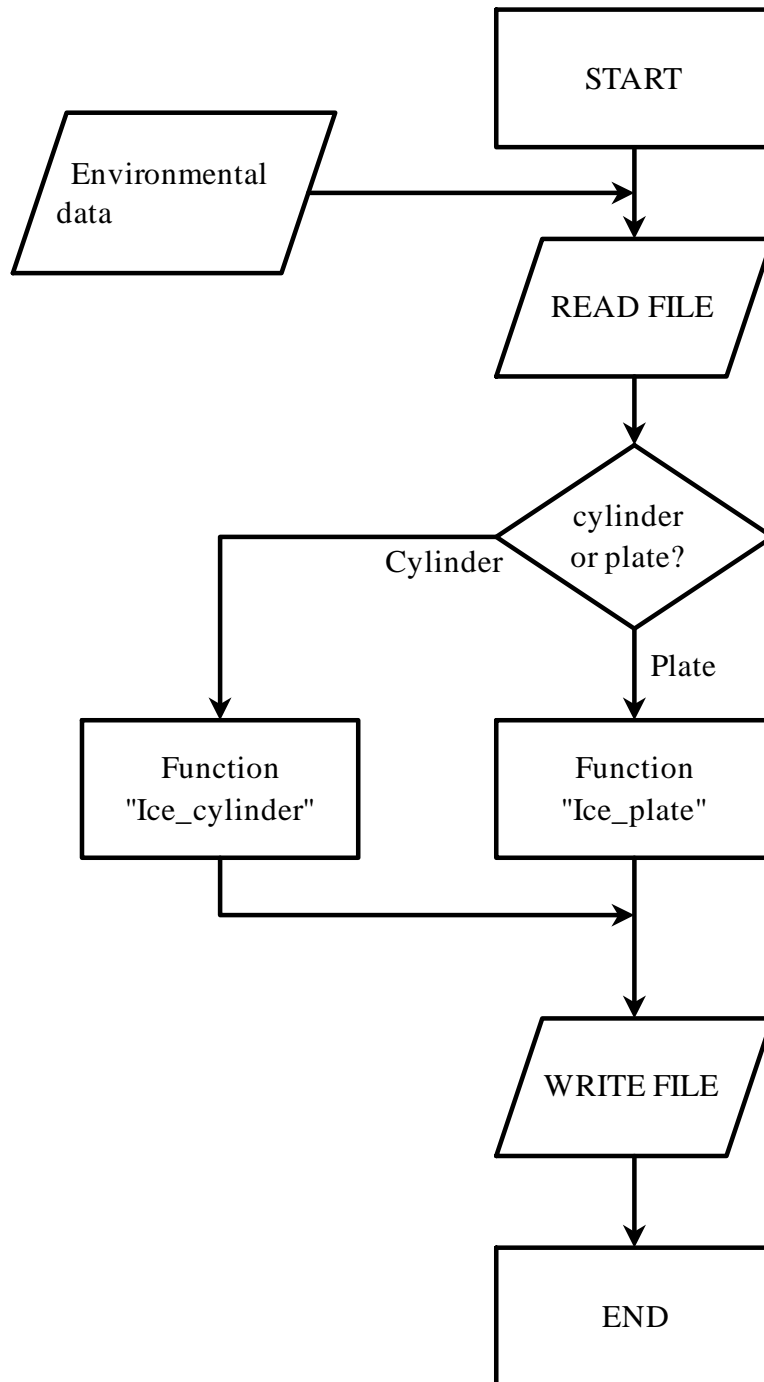
Figure 5.1 Flow chart for the whole computational process. First read file and compute based on given values and write the result out into new file. Each small cylinders and plates are calculated by different function.

5.2.2 Tailor Made Function: "Ice_cylinder" and "Ice_plate"

Icing speed/intensity is calculate in two empirical function aim to calculate icing rate, As stated in several research such as (Stallabrass 1980), (Horjen1983) iteration process is applied to estimate icing rate, i.e. ice thickness growing in an hour. See Figure 5.2. These calculation is based on empirical formulation explained in chapter 2.
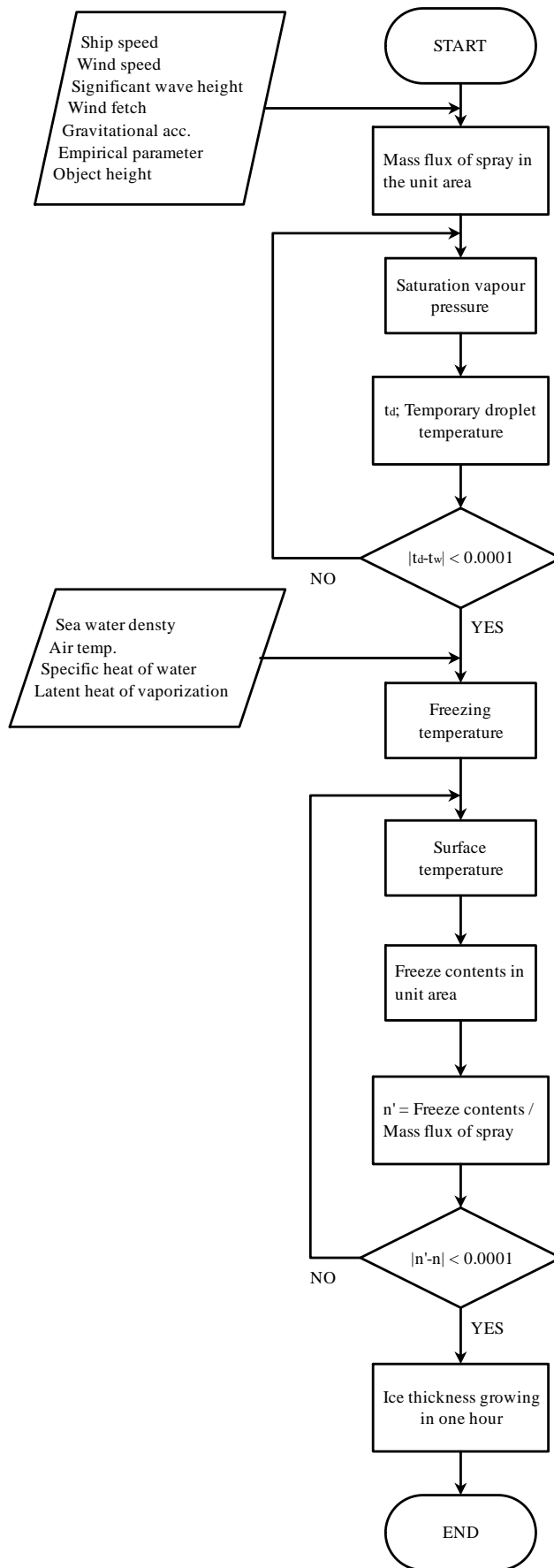
Figure 5.2 Flow chart for the computation of ice intensity, used on tailor made function "Ice_cylinder" and "Ice_plate". Iteration procedure is used twice, which is repeated until the difference of the successive value converges.

32

5.3 Simplified Ship's Shape and Superstructures

5.3.1 The Model Ship

In our computation 500 tonnage size of coast guard vessel is selected for our case study. The reasons why we chose this type of ship as an object of the model is:

1. Search and rescue on the severe weather conditions.
2. Rate of ice growing on the elements.
3. Relatively small size vessel; 500 [t] is vulnerable to the ice accretion.
4. Quantity of the data existing for the analysis of case study (e.g. Tabata 1963)

Regarding 1, disaster at harsh sea not only capsizing due to icing on extreme condition, there are potential dangers on the high north region that increase the necessity of a search and rescue operations by the coast guard vessels. That is why such vessels have to avoid getting ice build on the structure in order to implement safety operation in high competence at harsh condition. Those who engaged in the operations should have known such potential dangers.

With respect to 2, due to high speed operation; up to approx. 25 kts, the faster the higher icing rate, (ref chapter 2). This kind of high speed operation ship should be carefully prepared for icing.

With respect to 3, large vessels like VLCC are strong to icing, because even if ice accretes on the deck structures ice loads are much smaller than ship's displacement. That is why smaller ship has a potential to be affected by ice load, and stability change drastically due to additional load. The ship size of 500 tonnages is selected since its size ship will be operated on the sea exercise.

Regarding to 4, after the analysis is calculated for ice load and stability change it should be investigated by comparing with full scale tests.

A photo below shows an example of such kind of vessels; *M/V Yubali* of Japan Coast Guard.

Figure 5.3 *M/V Yubari* of Japan Coast Guard. Compare with Figure 5.4. (Photo source: http://www.panoramio.com/photo/42232495xz)

5.3.2 Simplification Method of the Ship Structures

From a practical view point it is impossible to consider all the structures on deck to include the ship icing simulations, especially for the prototype study it is not convenient. That is why as a beginning point of modelling, simplified ship shape is considered as shown in Figure 5.4.

Important thing that should be carefully considered is that degree of simplification should not being far away from original model otherwise the result will be useless whose values are far beyond from
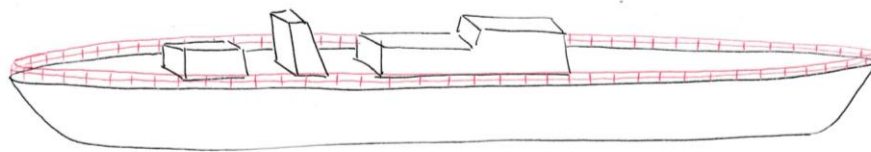
Figure 5.4 Model ship and simplified superstructure, hand rail and the front area of bridge is calculated on the simulation of ice accretion, except for it is simplified. Compare with Figure 5.3.

the result which they experience on the real situation and lead the model to be meaningless. This is a general rule of simplification.

For the simplification purpose most of the complicated ship structures with low dependency to the icing like life boats, funnel, windlass, must, radio communication lines, etc. are not calculated due to computational simplification reason. But the hand rails surrounding along the ship's brink will remain, in the Figure 5.4 it is shown by red lines, composed of vertical and horizontal bars. There are two ellipsoidal shape and 52 vertical bars length of 1 meter. Since LWC depends on height as shown in eq. (2.12), ice load on it is also height dependent, that is why in order to get more accurate result, those vertical bars should be calculated by cutting it into small pieces. When deciding the length of short element, we compare variation of LWC are height dependent in Figure 5.5. For comparison purpose 5 way to calculate LWC are shown referred in chapter 2. Although it is not easy to define appropriate length of element from this result, best thing is that integrate the vertical bars though not practical for the model which need fast computation time in terms of final goal is installing to ice bridge simulator. We shall judge that at least 10 cm element for the model will sufficiently compensate the difference and with its error of negligible level.
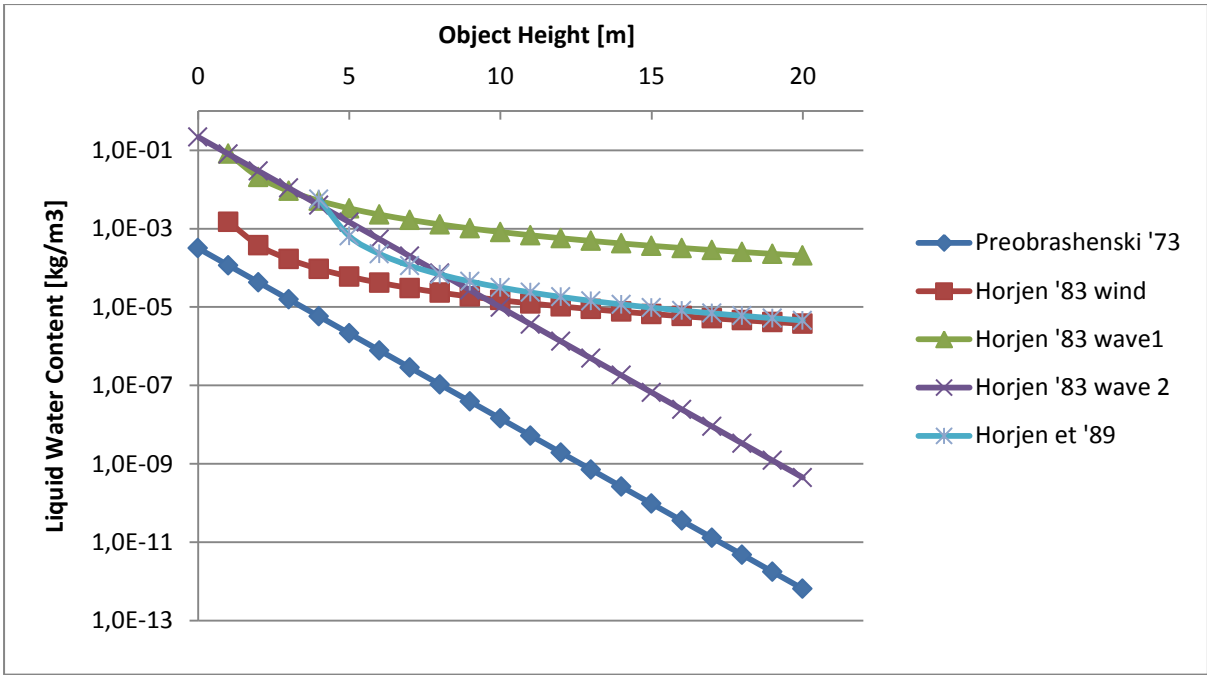
Figure 5.5 The vertical variation of LWC, wind speed 22 [m/s] and significant wave height 6.9 [m].

with the distance of approximately one meter separation. The diameter of these bars is 0.4m. From Figure 5.6 *M/V Yubali* we could clearly find that the icing on hand rail will lead to water trapped on deck due to the wall made by ice between horizontal hand rails.

Table 5.1 Ship's data table for the model ship on our simulation. We use same data of *M/V Yubari*. Data taken from Tabata et al. 1967.

Lpp	45.00 [m]
Breadth	7.30 [m]
Depth	4.10 [m]
Gross Tonnage	326.92 [t]
Initial GM	0.81 [m]
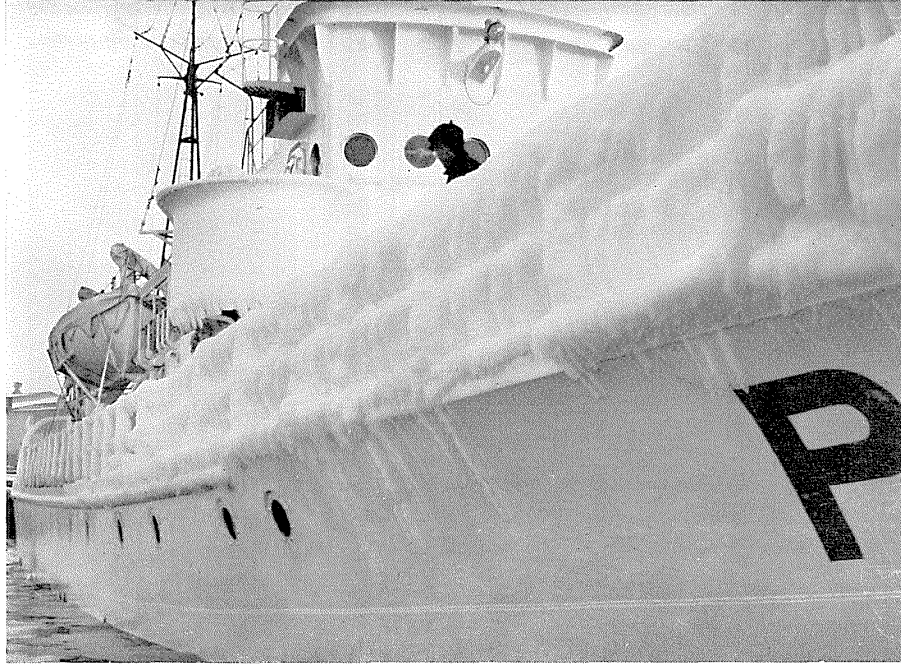
5.4 The Ice Formations between Horizontal Handrails

On the calculation of the simulation ice formation is assumed to be evenly formed around the cylinders and on the plates but it is not true according to the field test by Stallabrass 1967. The external force acting on the ice deforms it; gravitational force deforms the ice down sagging make icicle in case as shown in Figure 5.8, additionally this phenomenon contribute strongly make a wall between horizontal hand rails and let green water on deck not being escaped. In order to quantify it, we analyze the wind tunnel executed by Stallabrass et al. 1967. Also above figure is a good picture that opening is compensated by accreted ice. Figure 5.8 shows accreted ice on 3.8 cm diameter cylinder placed horizontally. The ice formation is extending downward due to gravitational force. We could find linear relation between weight of ice and dimension A and not depending on the air temperature and cylinder diameter, see Figure 5.9.

Evenly formed ice around cylinder
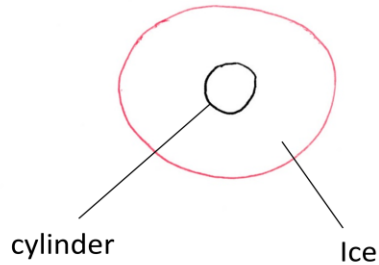
Deformed by gravitational force and wind

cylinder   Ice

A
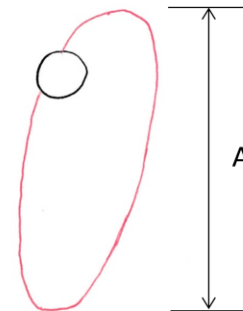
Figure 5.7 A image of the cross section of the ice accreted on the ship's hand rail. From Figure 5.8 we could fine that ice formation on the offshore field is like right hand image. The vertical length of the ice is expressed as a function of ice weight. The dimension A is refereed in Figure 2.6.

Table 5.2 The result of the wind tunnel test. Reproduction from Stallabrass 1967 Table I. This data is based on that of horizontal cylinder. Figure 5.9 is produced from this data set.

cylinder diameter [cm]	Air temp. [°C]	weight of ice [kg/m]	Dimension of ice formation at mid-span [cm]			
			A	B	C	D
3.8	-15	16.8	35.6	8.9	10.8	12.7
3.8	-8	9.0	16.5	5.1	7.6	10.2
7.6	-14	16.9	33	8.3	9.5	14
7.6	-7	11.4	22.9	5.1	8.3	8.3
15.2	-16	26.7	39.4	8.3	12.7	15.2
15.2	-7.5	15.5	29.2	5.1	9.5	10.2
30.5	-14	39.9	63.5	8.3	10.2	17.8
30.5	-10	27.1	48.3	5.1	10.2	12.7
45.7	-13	46.4	68.6	8.3	11.4	19.1
45.7	-9	32.4	55.9	3.8	7.6	12.7

Location of cylinder
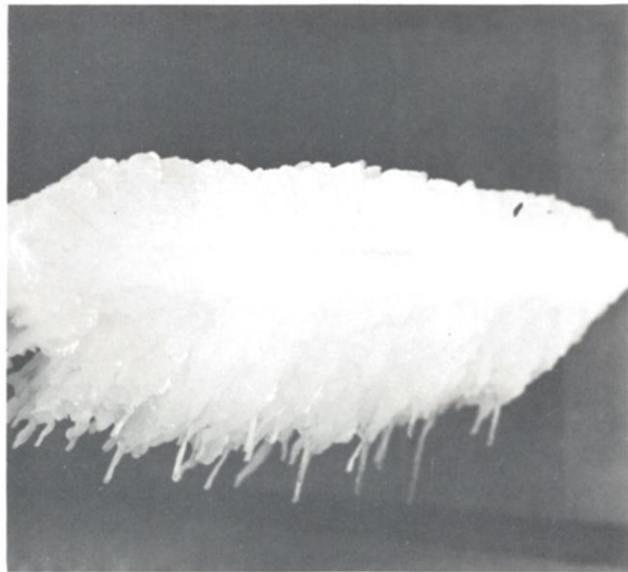
Cross section of ice

Air temperature -15°C
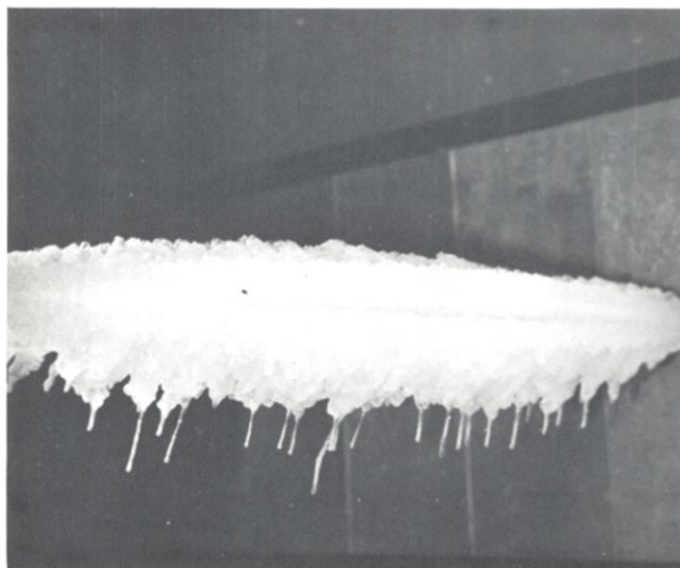
Air temperature -8°C

Figure 5.8 Ice accretions on 3.8 cm horizontal cylinder after 1 hour exposure (Stallabrass et al. 1967). Ice formation is completely made on windward side of the pole with icicles extending downward due to gravitational force.
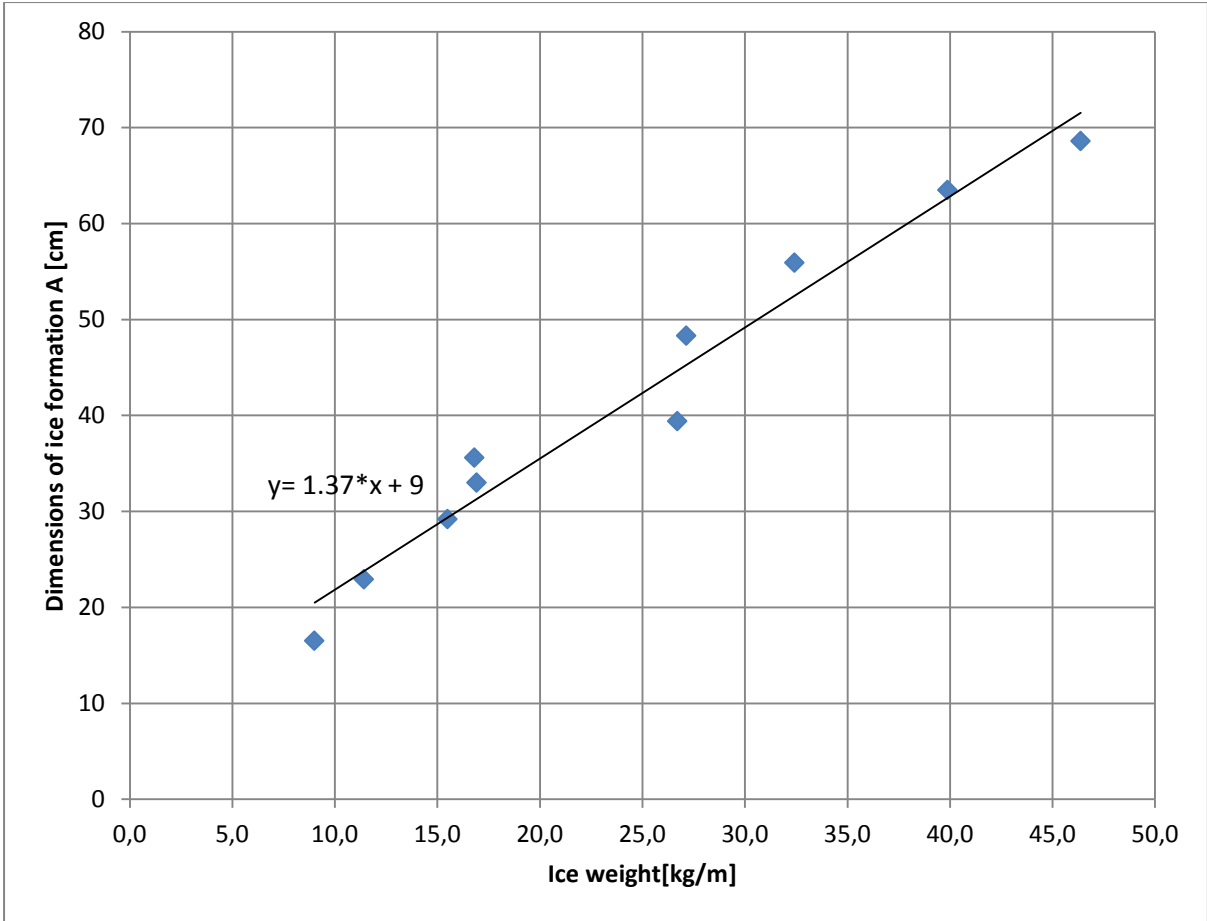
Figure 5.9 Length of dimension A is expressed as a function of ice weight, linear regression line is added. Length A can be expressed as a function of ice weight regardless of other parameters such as temperature and cylinder diameter.

As show in figure5.9, ice weight and vertical length A has linear relation;

$$A = 1.37 * w_i + 9 \qquad\qquad ; w_i > 10 \qquad\qquad (4.1)$$

where   A = length at the dimension A [cm]

w_i = ice weight around cylinder [kg/m]

but we have to be careful that if weight of ice is zero, length A will be 9 [cm] according to eq. (4.1), and that is not real case, so in the small ice weight the above expression cannot be applied as stated that "$w_i > 10$".

5.5 Validation of the function "Ice_cylinder" and "Ice_plate"

5.5.1 Selection of the Expression for the Mass Flux of Spray per Unit Area

As expressed in subchapter 2.2.2 LWC is estimated by several procedures. Estimation of LWC is difficult; it should be considered such that external condition and ship motion; wave height, wind speed, object height, and also ship speed, course as well. Comparison of those expressions and the way how to select reliable one is stated in the following.

39

Figure 5.10 shows LWC values as a function of wind speed, object height is fixed on 3 m which is average height of cylinder in our study.

Key findings are:

a) In case of Horjen et al '89 the LWC values suddenly grow up around the wind speed of 15 [m/s].

b) In case of "Horjen '83 wind" the numbers grow rapidly at the wind speed of 20 [m/s]. During the range of wind speed 0-5 [m/s] there is small undulations, this is because of third polynomial, see eq. (2.7).

c) Except for the Preobrazhenski '73 LWC value increase rapidly at a certain wind speed. It means the relation between wind speed and icing intensity is not a simple linear relation.(Neither exponential nor logarithmic relation)

d) The line of Horjen '83 wave 2 but around the wind speed 13 [m/s] and start again, this is because of the empirical constant change at that point. see chapter 2.2.2.

 Note; Icing rate will be depending on other parameter like air/sea temperature and wind speed, it is difficult to judge the validity of those expression or reliability. Although this figure shows the behaviour of it as a function of wind speed it is not easy to judge which expression to be used on for icing the icing model. There is room to be developed further analysis.

Additionally since LWC is a mass flux per unit volume, it is regardless in terms of if the object is plate or cylinder. That is why figure below does not contain parameter for plate or cylinder.
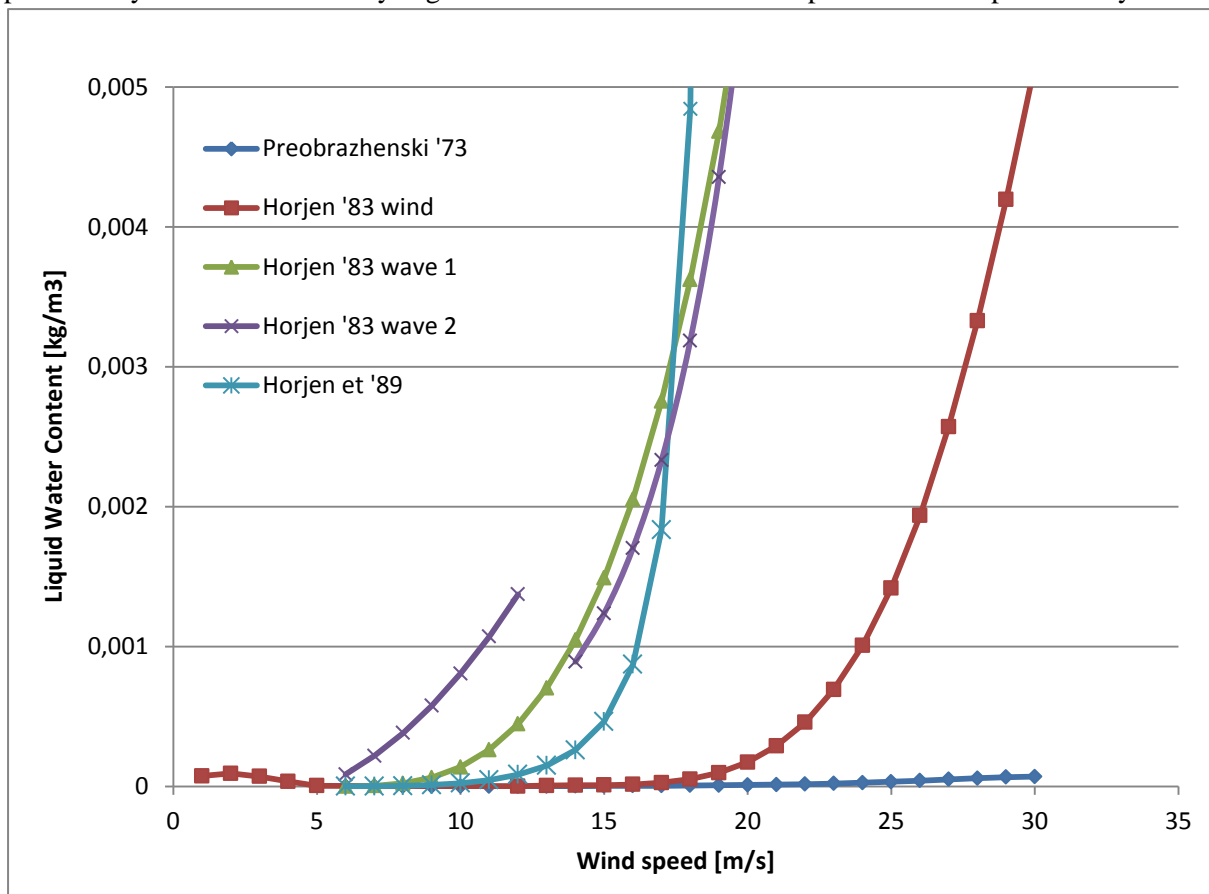
Figure 5.10 Liquid water content as a function of wind speed, the object height is set to 3 m form sea level which is typical height of handrail in proposed model.

5.2.2 Comparison with the Mertins' charts

In order to evaluate given model, one have to compare it with the field test result. The Mertins' charts (Figure 5.11) are shown as a field to be compared with. The figures are created by the Mertins' 1968 at Marine Weather Sectors in Hamburg from field observation of collected reports over 10 years period, distributed forms from recording ice observations from German and English fishing trawlers. (Mertins 1968) What we have to be careful on this chart is that this picture is expressed by those parameters such as "wind force", "air temperature", and "Sea temperature", not including "object height" and "characteristic length (e.g. cylinder diameter), which means this figure with ambiguous. But in terms of data reliability that those are made from more than 400 field data; it must be reliable enough for our investigation.

In order to compare with the Mertins' charts and proposed model shown in Figure 5.12 we have to make a same assumptions. Firstly we set use 0 °C for sea temperature, characteristic length as a cylinder diameter is set to 0.04 m, object height is 4m (For Beaufort scale 11-12, set wave height 6m), and significant wave height is derived from expressions on Appendix B (U.S. Naval Oceanographic Office 1966). The wind speed is taken by the middle value of the range, for instance in case of Beaufort scale 8; wind speed is 17-21 m/s so as 19 m/s shall be selected (Refer Table 2.2 *Beaufort scale*).

Although it is not easy to compare proposed model and Mertins' chart because of complexity of ship icing, we could write key findings:

   - In the Mertins' charts the ice thicknesses are expressed much larger than proposed model.

   - In the Mertins' charts values are not precisely fixed, have large range (e.g. 7-14 [cm/24hour]), alternatively proposed model shall calculate exact number.

   - The quantitative difference is not the difference of order, means that we could conclude that proposed model is not far from this field data.

   (More detail about quantitative analysis will be shown in appendix C)
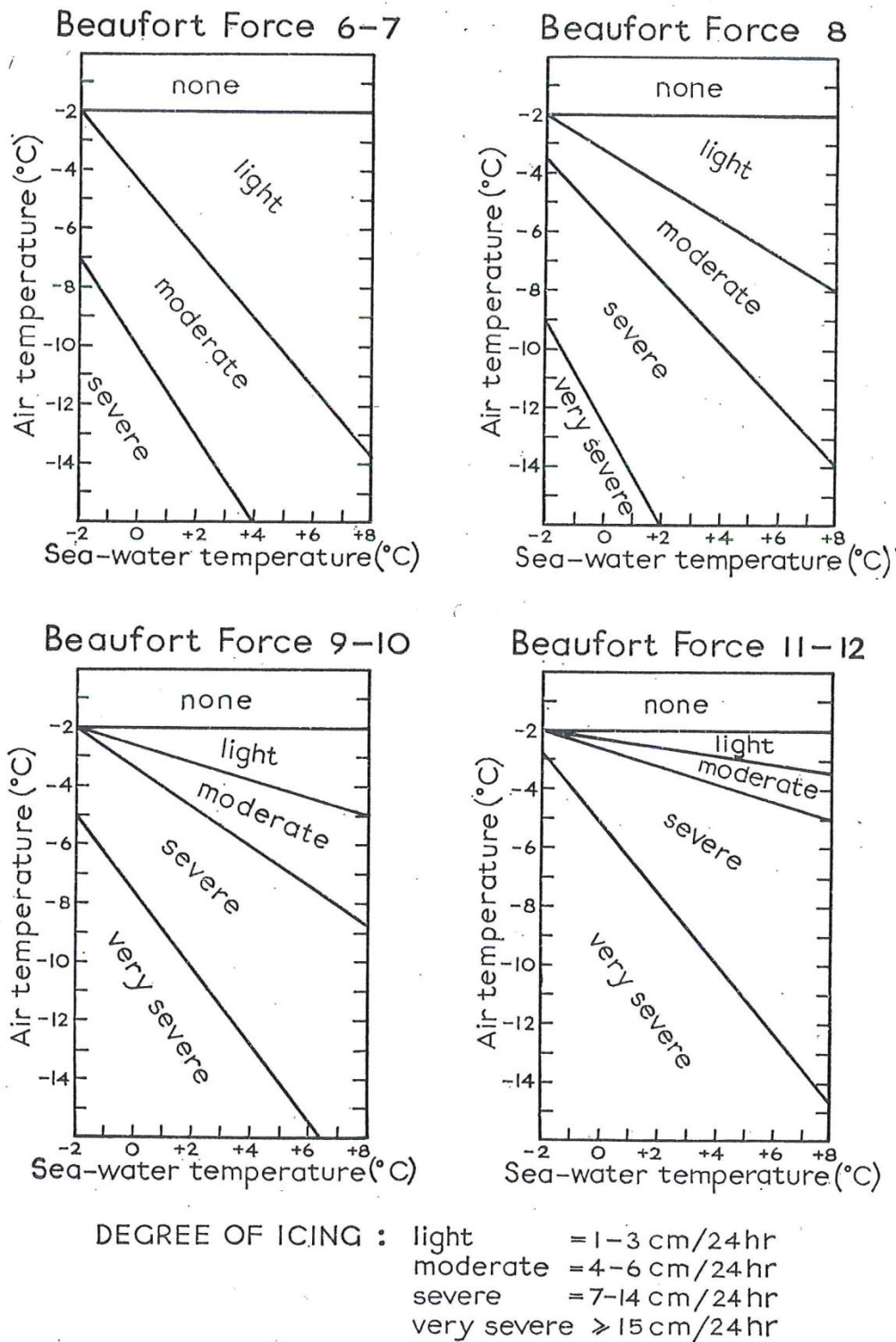
Figure 5.11 Mertins chart (from Mertins 1968). Icing rate (degree of icing) is expressed by air and sea temperature, composed of 4 figures according to wind force. These numbers are based on field data taken by Marine Weather Sectors in Hamgurg at the sea area of Ice land, Greenland, Labrador and Barents sea where significant icing can be observed ordinary.
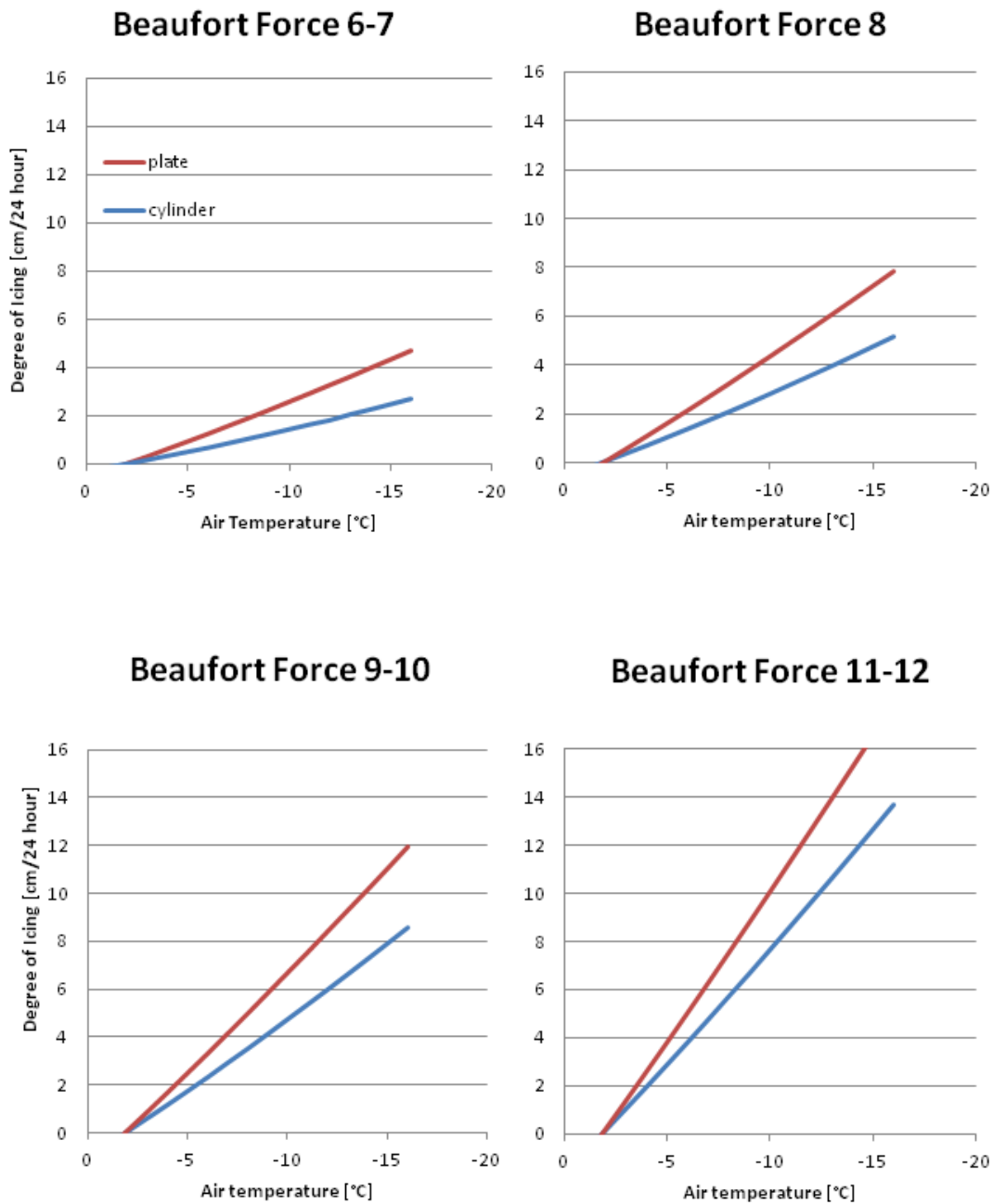
Figure 5.12 Icing rate [cm/24hr] as a function of air temperature to be compared to Figure 5.11. Sea temperature is fixed on 0 °C for simplification reason. The red shows the value of plate, blue square is for cylinder. Those two values make a difference if the air temperature decrease. Notice that right hand side is much lower temperature.

Chapter 6 Validation of the Ice Model

6.1 Introduction

In order to validate proposed model two case studies have been executed, one is compare with full scale test and the other is by setting external condition according to Beaufort scale. Because of complexity of ship icing it is not easy to validate model, so that proper amount of assumptions are necessary which we made for external conditions, also metacentric position not being affected by icing. Finally reliability of proposed model is discussed from operational view point. This section is of importance in terms of model reliability for the enhancement of training quality regards to the ship operations in the arctic regions.

6.2 Case Study

6.2.1 Case Study 1: Comparison with Full Scale Measurement

First we compare simulation result with that of field test examined at the offshore sight at the coast of the Northern Territories, Hokkaido, Japan. The data of full scale measurement are taken from Tabata 1963.

For a comparison purpose we assume following condition according to Figure 6.1. Since proposed model cannot simulate continuous change in time domain for those weather parameters like wind speed, wave height, etc have been set constant. These values are dealt by taking average value from full scales test report.

 [The weather conditions]

      - wind speed = 14 [m/s]

      - Significant wave height = 4.0 [m]

      - Air temperature = -7 [$^{\circ}$C]

      - Observed ice period = 20 [hour]

On deciding above test condition, we have set assumption that:

- Air temperature, wind speed, significant wave height is stable during the analysis on this case study, so as those values are constant and average value has been taken from Figure 6.1. (The doted area shows period that icing was observed, which summed up 20 hours. During three days examination, ship course, ship speed, wind speed and direction, sea state, weather, barometric pressure, air/sea temperatures are recorded with specific comment. Data were taken at January 1961, *M/V Yubari*.)
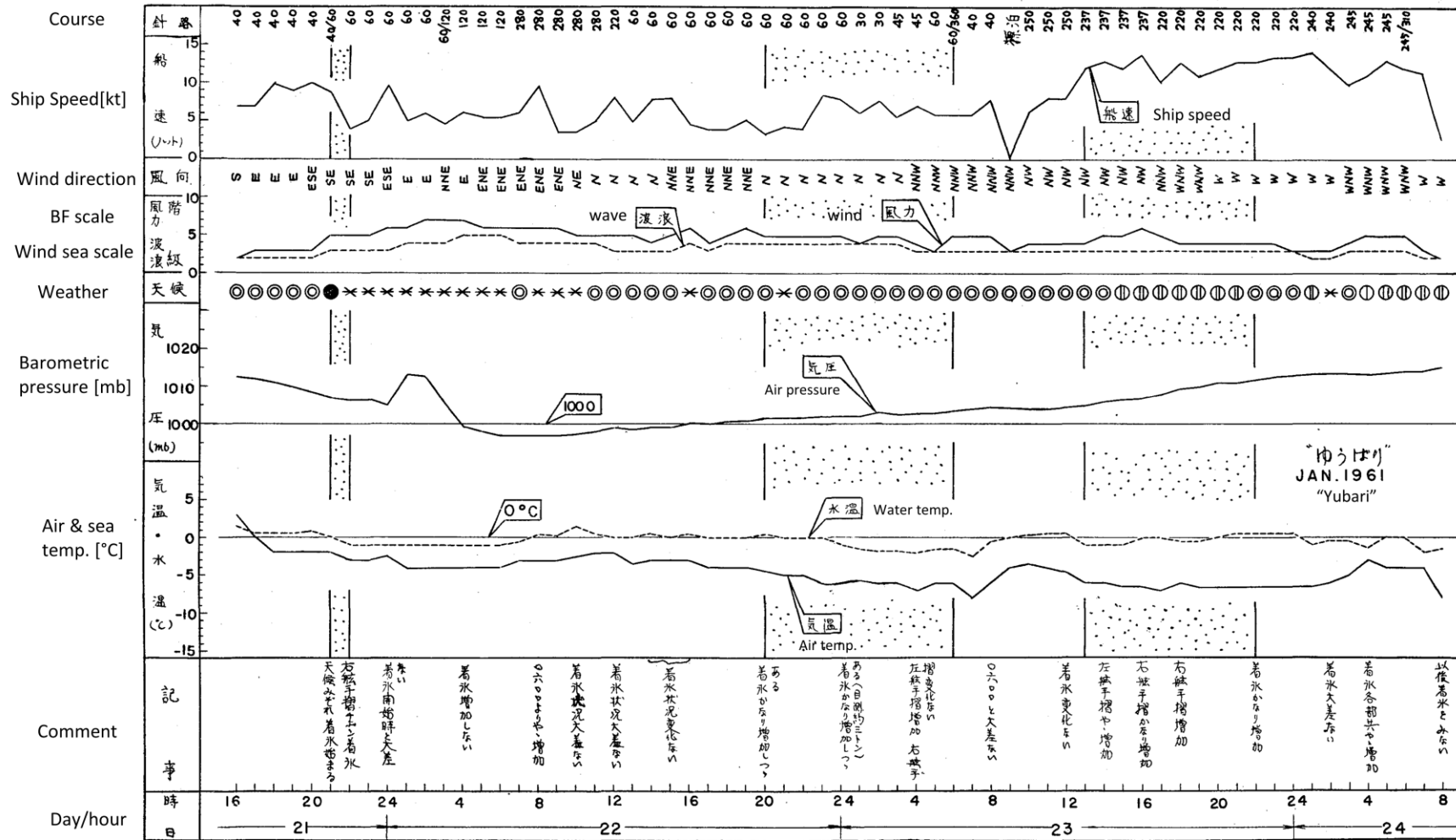
Figure 6.1 Field condition, wind, wave, ship speed, direction, etc. Those dotted area explain period when significant icing is happening. The comments in most below column are by navigational officers on board, notification is written in Japanese. From this figure we could find that icing is depends not only air temperature, but also ship speed, ship course; i.e. relative wind contribution is of importance.

45

The simulated ice load in time domain is shown in Figure 6.2. Ice load increase as time goes with the inclination become steep because of the ice diameter getting larger. The total ice load after twelve hours test/simulation is shown in table 6.1. Also the KG and GM values; both for before icing and after icing is on Table 6.2. The final ice load after 20 hours operation differ 2.2 [tonne], the GM change differ 0.03 [m]. The rolling period differ 0.14 [sec] that human cannot perceive it.

Note that we assumes in our simulation that the metacentre position has not been affected by ice load, (difference of KG and GM for full scale test differ 0.01 m) so that GM is simply calculated by KG change if we know initial metacentric position (KM), i.e.:

$$GM = KM - KG \qquad (6.1)$$

where KM is found from data sheet in Tabata 1963.

For further inspection of this model, rolling period is compared (Table 6.2). The rolling period is given by,

$$T = \frac{2\pi K}{\sqrt{gGM}} \qquad (6.2)$$

where K is radius of gyration which is depending on breadth and given by K=CB, C is approximately known as 0.4 in this type of ship, B is ship's breadth, Table 6.2 can be obtained (Tabata 1963).
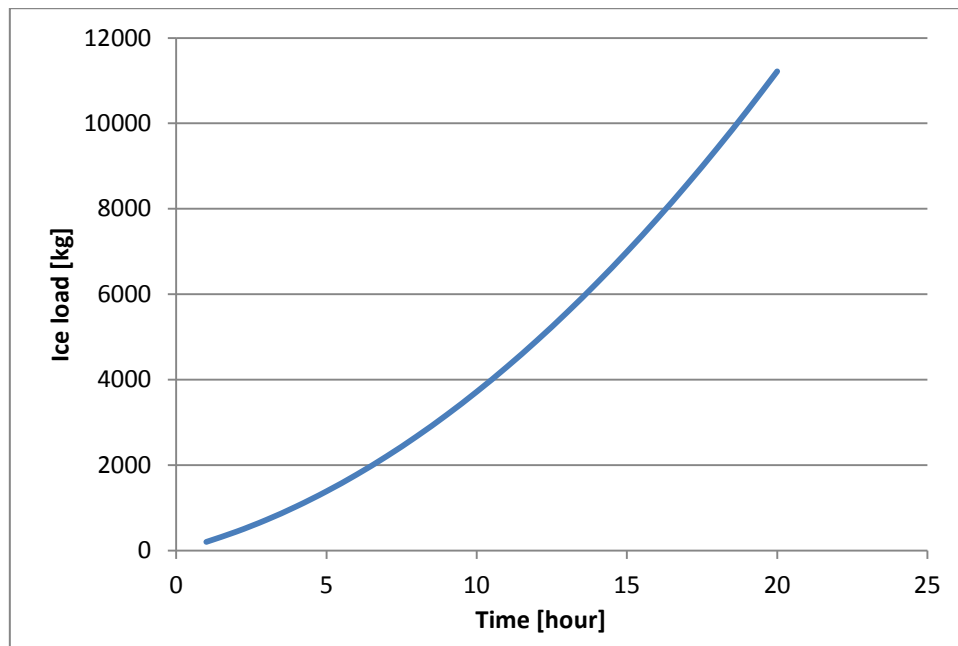
Figure 6.2 Simulation result of the case study for comparison with Tabata's full scale test. Ice load increases as time goes with the inclination also be steep, this is because of the fact that even if icing rate is same the diameter of the cylinder become large.

Table 6.1 compare resultant ice load. The difference is around 2.2 tonnes.

	Ice load [t]
Field test	13.388
Simulation	11.217

	Before icing	After icing	difference
	Full scale test		
KG [m]	2.67	2.75	+0.08
GM [m]	0.81	0.72	-0.09
T [sec]	6.51	6.90	+0.39
	Simulation		
KG [m]	2.67	2.73	+0.06
GM [m]	0.81	0.75	-0.06
T [sec]	6.51	6.76	+0.25

6.2.2 Case Study 2: Different Sea State in Accordance with Beaufort Scale

In this analysis we define three conditions according to Beaufort scale (ref Table 2.1), followed by relative wind speed and significant wave height is derived from U.S. naval Oceanographic Office (U.S. NOO 1966, also see appendix B), for air temperature -5, -10 and -15 degree Celsius are selected respectively, case 3 is most severe and case 1 is most moderate sea state. Detail analysis results are shown below.

Table 6.3 Test condition for case study 2. Significant wave height is estimated by the polynomial of U.S. navy. Air temperature is selected arbitrary to make the significance of the result.

	Condition 1	Condition 2	Condition 3
Beaufort scale	3	6	9
Relative wind speed [m/s]	4.6	13.0	23.0
Significant wave height [m]	0.5	2.9	7.4
Air temperature [°C]	-5	-10	-15

GM height is calculated and result is shown in Figure 6.3. Note that GM is calculated under assumption that metacentric height KM changes much small enough compared to ship dimension during icing as well as case 1, difference between KG and KM is 1 [cm]. KG is calculated by eq. (5.1).

From Figure 6.3 case 1 and case 2 had difference of 4 [cm] regard to this point we could say that in these sea state there are no strong influence toward stability for this type of ship in 20 hours operation. Alternatively BF9 GM differ 25 [cm] and make significant stability reduction.

A typical working value of GM is shown in table 6.4 in order to be compared with resultant GM.
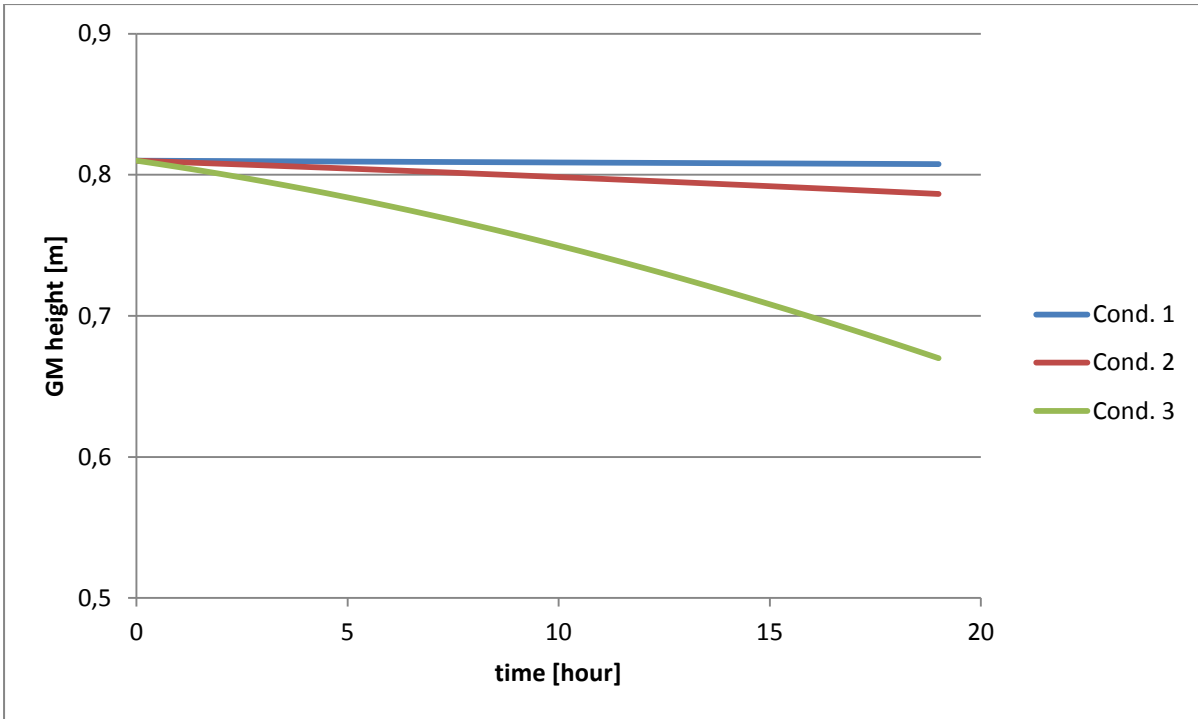
Figure 6.3 GM height, simulation result, the more harsh condition the larger change of GM can be observed. Note in case of condition 3 GM has reduced to 80% from the initial values. There are small difference between cond. 1 and cond. 2.
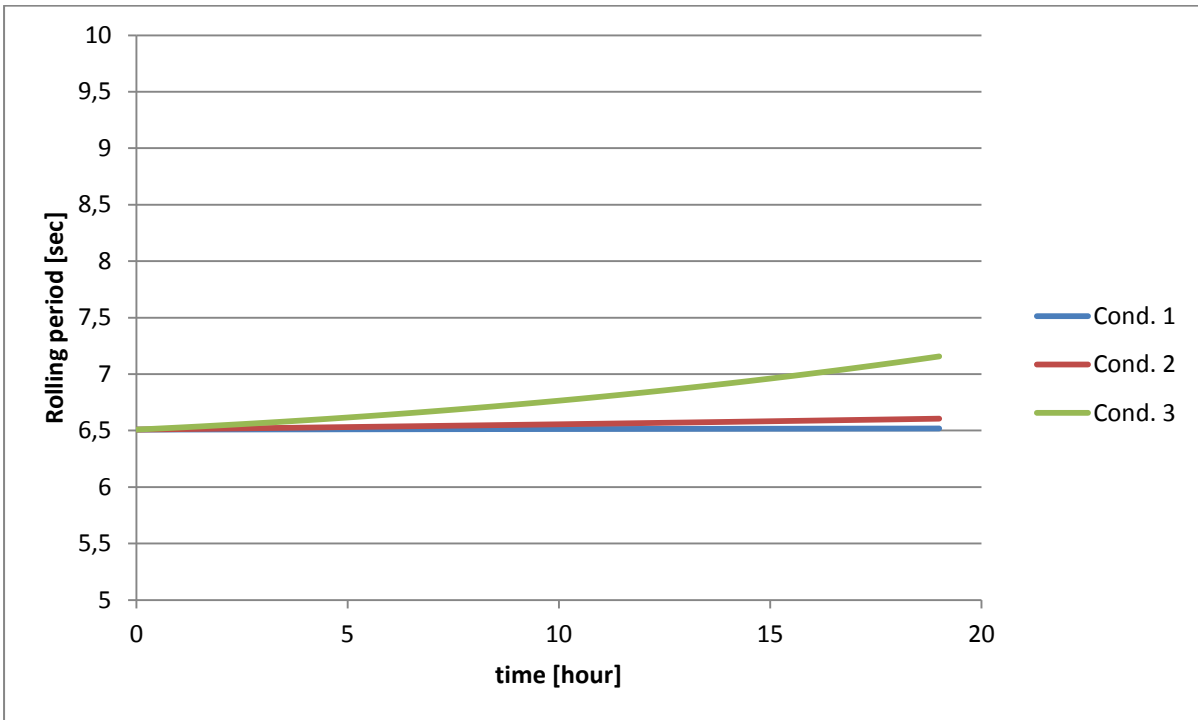
Figure 6.4 Rolling period according to assumed conditions. In case 1 and case 2 difference is approximately 0.1 sec, case 3 will make more than 0.5 [sec] difference on the duration of 20 hours. Point is if the ship navigator can notify the change of rolling period.
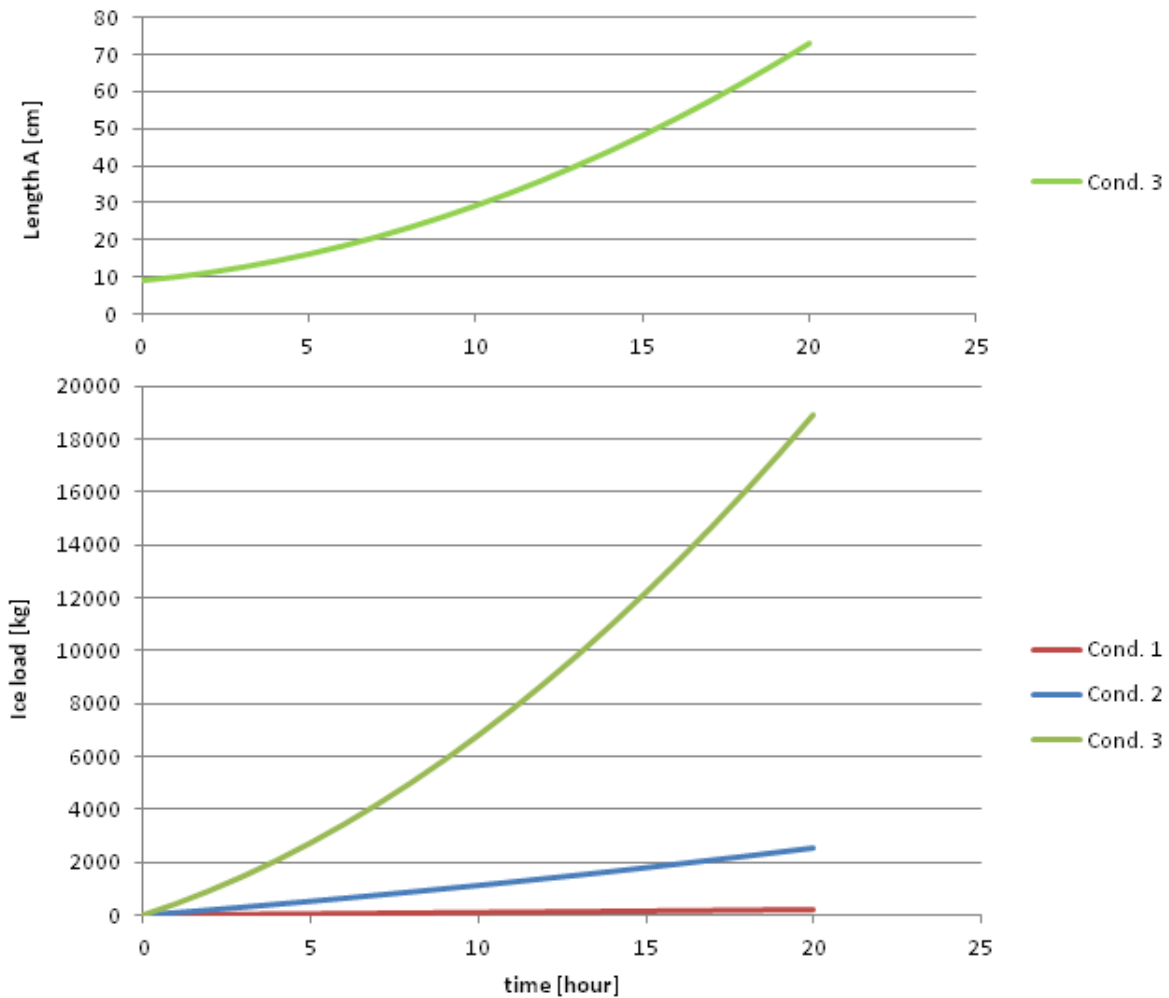
Figure 6.5 Simulation result of ice load of Case study 2. Ice load (below) and length A for Cond. 3(above) are shown. The black dotted line is the length between two vertical handrails, if this value exceeds this line sudden stability can be observed due to trapped water on deck.

Table 6.4 Typical working values for GM for several ship-types all at fully-loaded drought. Reproduction from Barrass 2006. The subjected ship in proposed model is similar to "General cargo ship".

Ship type	GM at fully-loaded condition
General cargo ships	0.30-0.50 [m]
Oil tankers	0.50-2.00 [m]
Double-hull supertankers	2.00-5.00 [m]
Container ships	1.50-2.50 [m]
Ro-Ro vessels	1.50 [m] approximately
Bulk ore carriers	2-3 [m]

Since in this model the opening between hand rails are 50 [cm], during operation under condition like case 3, 16 hours later from initial icing trapped water could not escape from ship's deck and sudden stability change is observed. Hence when one install this model to the bridge simulators, the length A should be indicated on Bridge instrument or to be visualized in display so that navigator could find if the ship has potential of sudden stability change due to trapped water on deck.

We have to note about mass flux per unit area "G(z)" in the code eq (2.12). Since this function has a limitation of object height; $z > \frac{1}{2}H_s$ which is not suitable for icing calculation in terms of wall making because if there are no icing observed at this height in severe sea state, the wall cannot be constructed. Hence we use other expression for "G(z)" such that (Stallabrass 1980):

$$G(z) = 1.7 \cdot 10^{-4} H_s U \tag{6.1}$$

This expression is based on his own calibration by comparing with observed field data, moreover original formulation was suggested by Kachurin (Stallabrass 1980).

The trapped water problem and when it occurs

If the ship operates in the severe sea condition, surrounded hand rail will make a temporary wall that traps green water on deck causing sudden stability change due to its free motion on deck (Chapter 3.2). In our simplified model those hand rail has opening of 50 cm spacing vertically. So we can say if those openings are completely filled with accreted ice walls are constructed. In our case study such conditions are observed after 16 hours continuous icing simulation.

6.3 Validation of the Ice Model

Case studies have shown in previous sub chapter. Here the model is validated.

For case study 1 assumption is taken by average value of field data though, final ice weight shows quite similar value. The difference is from Table 5.1, approximately 2.2 tonnes, this is if we compare with the ship's displacement of 326.9, it is 0.67% and not large influence to those stability parameters. Similarly about GM change both for 20 hours operation and simulation as shown in Table 5.2 the difference -0.09 for full scale test and -0.06 and the difference is 3 [cm] and if we get output as rolling period will be calculate 0.1 [sec] by equation (3.1) which is negligible in terms of human perception ability.

From case study 2 as expressed in Figure 6.3 for Cond. 1 and Cond. 2 there are not so large change of GM and also rolling period is within such that navigational officers cannot notice its periodical change. But for Cond.3 GM change 15 [cm] which makes change to rolling period (0.6 [sec]) compared to other condition this number is large though, doubt that if human can notice is still remaining. Moreover in our case ice washed away due to green water is not calculated.

Also about radius of gyration K, we assume that is not change though it will change. But the change of $C = K / B$ will change from 0.402 to 0.393 in case of "M/V Yubari" for before and after icing respectively. By using equation (3.1) the resultant T differ -0.4 [sec], since if icing we have the rolling period increase and this difference -0.4 cancel it, which is negative effect for us, so if one need more precise calculation result this effect should be considered.

6.4 Discussion

Degree of simplification

We have made an assumption of the model and ship superstructure as shown in chapter 5.4. We have to discuss about whether the assumption is under affordable limit or not. From Case study 1, the final ice load differ 2.2 tonnes which is 0.67% of total ship's weight, and we can say this model has made an affordable degree of simplification. Note that for calibration purpose droplet diameter is set to 0.001 [mm]. In terms of GM followed by rolling period it change 0.1 [sec], note that rolling period has small correlation with GM, so we could not say anything from this number.

For Case study 2, since we don't have full scale test result for this case study that we cannot compare with.

Analysis method, condition setting

For Case study 1 we analyse the model by using constant values as an input of external condition by taking average values from Figure 6.1, but in order to get more reliable and continuous result for changing weather parameter those algorithm have to be time dependent, in other word it should be dynamic model. In this point those computer code should be modified. Regarding to calculation method of GM, we assume that metacentric point is not affected by ice load, but it changes (Tabata 1963). In order to obtain more precise one we can use hydrostatic table which is specific to ships that we could not obtain from literatures.

For Case study 2 the weather condition is defined by Beaufort scale followed by wind speed and significant wave height, but the air temperature is decided according to severity of the sea state, the

more severe sea state the colder to magnify difference of result. Alternatively the sea temperature is fixed to 0 °C.

For more investigation another full scale test should be compared with, unfortunately so far no full scale test has been done except for Tabata 1963 on Case study 1. The reason is the nature of complexity and quantification difficulty of ship icing.

Free surface effect and stability reduction

In our simulation the opening between vertical hand rails has been compensated during the operation on the condition 3. It means our simulation could make criteria on judging if subjected ship will experience sudden stability reduction in terms of "when". That is why from proposed model can also be able to applied for safety criteria of those ships operating the area such that cold and harsh conditions can be predicted. During simulation training this ice compensation could be introduced as a safety criteria, for instance introduce a display to show ice length of dimension A (vertical length of the ice on handrail), so that navigation officers can check if own ship is threatened by free surface effect thanks to green water on deck. Additional criteria that show possibility of the green water such as function of wave height and free board should be prepared at the same time.

Chapter 7 Concluding Remarks

6.1 Conclusion

Because of increasing activities in the high north region the demand of developed ice model for bridge simulator is necessary in terms of training of qualified ship navigational officers. On the arctic navigations additional precautions such that ship-to-ice interaction and structure icing shall be taken. Regarding latter term is of importance since causing stability change and capsizing in the worst case. Our aim of this thesis has been to compose more realistic model and install it to ice bridge simulators for safer arctic maritime operations.

Both quantitative and qualitative literatures have been surveyed in the initial stage of this work, from those empirical and theoretical models, developed ice model to include important parameters with empirically obtained coefficients for build-up ice have been designed by using the computer language C++.

As a result of the development the ice model could include several external conditions for ice load calculations, and following GM is obtained for constant values of those parameters. The reality judgment of the model is not easy though from case study 1 the rolling period differ 0.14 sec compared to full scale result, from this number we could say that this model is not far from practice. Although installation of this model will be on the future work, the simulator training will be more reliable and proposed model contribute to increase training quality, following enhancement of arctic maritime operations.

By using obtained icing rate [mm/h] and considering deformation of the ice due to gravitational force and wind, range of the opening between horizontal hand rails can be displayed, and time domain data could show us when ship experiences sudden stability reduction due to trapped water on deck. From this view point we could conclude that by using proposed model notification of the sudden stability reduction to simulation trainee will be possible on a given conditions.

In this study prototype of ship icing model has been constructed by C++ based on both theoretical model and empirical data. As a result GM height and following rolling period in time domain can be calculated at the same time considering several external parameters which is not included in the current ice module. That is why we could say more realistic model has been proposed.

6.2 Recommendations for Future Work

Although prototype of developed ice model has been constructed it should be installed into existing ice bridge simulators. Strong collaboration with system engineers of the simulator manufacturer would be necessary to accomplish this work. One key task will be the visualization of the accreted ice for simulator training. The coordinate data of the ship mathematical model should link to ice module since the degree of ice differs depending on the structure geometry.

As a starting point we simplified ship shape and structures as Figure 5.4. The bridge simulators have several mathematical model of ship and the simplified shape shall be developed toward complex/real shape. In order to obtain more specific result it should be developed to come close to the real model.

Our algorithm is based on static analysis in terms of external conditions. Since those parameters such that relative wind speed, air temperature etc. are continuously change, dynamic model should be developed.

We have analyzed several methods to calculate LWC given by external parameters; in the case study we use simple estimation method that is not dependent on object height for the analysis purpose. Since LWC must be depending on not only wave height but also ship interaction with wave, these formulation have to be further studied to approach practical numbers.

Reference

Barrass, C. B. and Derrett, D. R. (2006): *Ship Stability for Masters and Mates. Sixth edition*, Elsevier.

Chung, K. K., Lozowski, E. P., Zakrezewski, W. P., Thompson, T. and Gagnon, R. (1995): *A Model for Spraying and Three-dimentional Icing on a Stern Trawler.* OMAE, volum IV, Arctic/Polar Technology, ASME 1995.

Handbook of Oceanographic Tables(1966): U.S. Naval Oceanographic Office, Washington, D.C. 20390.

Horjen, I. (1980): *A Survey of the Mechanical Properties of Sea Ice*, Marine Structures and Ships in Ice (MSSI), Report No. 80-01, 156p.

Horjen, I. (1981): *Ice Accretions on Ships and Marine Structure*, Marine Structures and Ships in Ice (MSSI), Report No. 81-02, 119p.

Horjen, I. (1983): *Mobile Platform Stability*, MOPS Subproject 02 – Icing, MOPS report No. 7. Norwegian Hydrodynamic Laboratories, NHL 283021.

Horjen, I. and Vefsnmo, S. (1984): *Mobile Platform Stability*, MOPS Subproject 02 – Icing, MOPS report No. 15. Norwegian Hydrodynamic Laboratories, NHL 84002.

Jones, D. F. and Andreas E. L. (2009): *Sea Spray Icing of Drilling and Production Platforms.* Cold Regions Research and Engineering Laboratory, ERDC/CRREL TR-09-3.

Lai, R. J. and Shemdin, O. H. (1974): *Laboratory Study of the Generation of Spray Over Water.* J. of Geophysical Research, Vol. 79, No. 21, pp. 3055-3603.

Makkonen, L. (1984): *Atmospheric Icing on Sea Structures.* U.S. Army Cold Regions Research and Engineering Laboratory Monograph 84-2, 102pp.

Monahan, E. C. (1968): *Sea Spray as a Function of Low Elevation Wind Speed.* J. of Geophysical Research, Vol. 73, No. 4, pp. 1127-1137.

Ono, N. (1964): *Studies on The Ice Accumulation on Ships II. – On the Conditions for the Formation of Ice and the Rate of Icing.* Low Temperature Science, Series A, Physical Sciences, 22: 171-181.

Ono, N. (1974): *Studies on Ice Accumulation on Ships. IV. – Statistical Analysis of Ship-Icing Conditions.* Low Temperature Science, Series A, Physical Sciences, 32: 235-242.

Overland, J. E. et. al (1986): *Prediction of Vessel Icing.* Journal of Climate and Applied Meteorology, Vol. 25, No.12, 1986.

Overland, J. E. (1990): *Prediction of Vessel Icing for Near-Freezing Sea Temperatures.* Weather and Forecasting, Vol. 5, pp. 62-77.

Rohsenow, W.M. and Choi, H.Y. (1961): *Heat, Mass, and Momentum Transfer.* Prentice-Hall, Inc.

Stallabrass, J. R. and Hearty, P. F. (1967): *The Icing of Cylinders in Condition of Simulated Freezing Sea Spray.*N.R.C.Mechanical Engineering Report MD-50, N.R.C. No. 9782.

Stallabrass, J.R. (1970): *Method for the Alleviation of Ship Icing. Mechanical Engineering Report MD-51,* National Research Council of Canada.

Stallabrass, J. R. (1980): *Trawler Icing. A compilation of work done at N.R.C.* Mechanical Engineering Report MD-56, N.R.C. No. 19372.

Tabata, T., Iwata, S. and Ono, N. (1963): *Studies on the Ice Accumulation on Ships I.* Low Temperature Science, Series A, Physical Sciences, 21: 173-221.

Tabata, T. (1968): *Research on Prevention of Ship Icing.* Institute of Low Temperature Science, Hokkaido University, Translated by Hope, E.R. Defence Scientific Information Service ERB Canada.

Tabata, T. (1969): *Studies on the Ice Accumulation on Ships III.* Low Temperature Science, Series A, Physical Sciences, 27: 339-349.

Zakrzewski, P. W. (1986): *Icing of Ships. Part I: Splashing a Ship with Spray.* National Oceanic and Atmospheric Administration, Technical Memorandum ERL PMEL-66.

Zakrzewski, W. P. (1986): *Splashing a Ship with Collision-generated Spray.* Cold Region Science and Technology, 14, 65-83.

Zakrzewski, W.P., Lozowski, E.P. and Muggeridge, D. (1988): *Estimating the Extent of the Spraying Zone on a Sea-going Ship.* Ocean Engineering, Vol. 15, No 5, pp. 413-429.

Appendix A
Collection Efficiency

Collection efficiency is a number between 0 and 1 that is the portion of the mass of droplets that are swept out by the cylinder that actually hit the cylinder, thus non dimensional parameter. The simplified collection efficiency for cylinder is expressed as the formula (Stallabrass, 1980);

$$E_c = \frac{\zeta - 3200}{\zeta + 27000} \qquad \text{if} \qquad \zeta \geq 3200 \qquad\qquad (A.1)$$

$$E_c = 0 \qquad \text{if} \qquad \zeta < 3200 \qquad\qquad (A.2)$$

The collection efficiency of rectangular body is expressed as

$$E_c = \frac{\zeta - 2800}{\zeta + 11700} \qquad \text{if} \qquad \zeta \geq 2800 \qquad\qquad (A.3)$$

$$E_c = 0 \qquad \text{if} \qquad \zeta < 2800 \qquad\qquad (A.4)$$

This is only if all the droplet are the same size, parameter

where $\varsigma = \dfrac{U^{0.6} d^{1.6}}{D}$

where   U = wind speed relative to the object [m/s]

d = droplet diameter [μm]

D = cylinder diameter or body width [m]

The collection efficiency increases with relative velocity, and with drop size, and decreases with the size of the object on which the drop impinge. Because the size of the water drops involved in ship icing due to sea spray is large, they will be deflected little and the collection efficiency will be assumed to be 100%.

Appendix B

Prediction of the significant wave height

The significant wave height is found as a function of wind speed and fetch (a distance over which the wind blow) as third- and fifth- polynomial which is valid for wind speed up to 32.4 m/s, which is taken from Handbook of Oceanographic Tables 1966.

$$H_s(U) = B_0 + B_1 U + B_2 U^2 + B_3 U^3 \qquad \text{[m]} \qquad (B.1)$$

$$H_s(U) = B_0 + B_1 U + B_2 U^2 + B_3 U^3 + B_4 U^4 + B_5 U^5 \qquad \text{[m]} \qquad (B.2)$$

Table B.1 Constant for third degree of polynomial of the wind speed given by equation above.

Fetch (n.m.)	B_0	B_1	B_2	B_3
100	$6.05709 \cdot 10^{-2}$	$2.89125 \cdot 10^{-2}$	$2.54698 \cdot 10^{-2}$	$-4.89792 \cdot 10^{-4}$
200	$4.21968 \cdot 10^{-1}$	$-7.75092 \cdot 10^{-2}$	$3.46928 \cdot 10^{-2}$	$-5.72020 \cdot 10^{-4}$
300	1.28311	$-2.26480 \cdot 10^{-2}$	$4.19756 \cdot 10^{-2}$	$-6.05377 \cdot 10^{-4}$
400	$6.09959 \cdot 10^{-1}$	$-1.32694 \cdot 10^{-1}$	$3.87922 \cdot 10^{-2}$	$-5.44265 \cdot 10^{-4}$
500	$5.59229 \cdot 10^{-1}$	$-1.34134 \cdot 10^{-1}$	$4.03976 \cdot 10^{-2}$	$-5.73259 \cdot 10^{-4}$

Table B.2 Constant for fifth degree of polynomial of the wind speed given by equation above.

Fetch (n.m.)	B_0	B_1	B_2	B_3	B_4	B_5
100	$8.68869 \cdot 10^{-1}$	$-4.41178 \cdot 10^{-1}$	$1.16227 \cdot 10^{-1}$	$-7.87593 \cdot 10^{-3}$	$2.62150 \cdot 10^{-4}$	$-3.34401 \cdot 10^{-6}$
200	$-7.71688 \cdot 10^{-1}$	$2.71899 \cdot 10^{-1}$	$1.07151 \cdot 10^{-2}$	$-8.30642 \cdot 10^{-4}$	$5.99481 \cdot 10^{-5}$	$-1.20460 \cdot 10^{-6}$
300	-2.31314	$5.96961 \cdot 10^{-1}$	$-1.71261 \cdot 10^{-3}$	$-1.75507 \cdot 10^{-3}$	$1.32954 \cdot 10^{-4}$	$-2.40288 \cdot 10^{-6}$
400	$4.86322 \cdot 10^{-1}$	$-3.41913 \cdot 10^{-1}$	$1.14635 \cdot 10^{-1}$	$-8.51850 \cdot 10^{-3}$	$3.24417 \cdot 10^{-4}$	$-4.49695 \cdot 10^{-6}$
500	$6.55261 \cdot 10^{-1}$	$-3.78443 \cdot 10^{-1}$	$1.11329 \cdot 10^{-1}$	$-7.55389 \cdot 10^{-3}$	$2.75507 \cdot 10^{-4}$	$-3.75483 \cdot 10^{-6}$

Appendix C

Comparison between proposed model and Mertins' Charts

In order to investigate proposed model, it should be compared with real numbers. See chapter 4.4. Here detail comparison result is shown below. These numbers are based on Figure 5.11 and Figure 5.12. See chapter 5.5.

Beaufort scale 6-7

	Mertins chart	Proposed model
Air temp = -5	4-6 [cm/24 hour]	0.5 [cm/24 hour]
Air temp = -10	7-14 [cm/24 hour]	1.5 [cm/24 hour]
Air temp = -15	7-14 [cm/24 hour]	2.5 [cm/24 hour]

Beaufort scale 8

	Mertins chart	Proposed model
Air temp = -5	7-14 [cm/24 hour]	1.0 [cm/24 hour]
Air temp = -10	7-14 [cm/24 hour]	3.0 [cm/24 hour]
Air temp = -15	>15 [cm/24 hour]	5.0 [cm/24 hour]

Beaufort scale 9-10

	Mertins chart	Proposed model
Air temp = -5	7-14 [cm/24 hour]	2.0 [cm/24 hour]
Air temp = -10	>15 [cm/24 hour]	4.5 [cm/24 hour]
Air temp = -15	>15 [cm/24 hour]	8.0 [cm/24 hour]

Beaufort scale 11-12

	Mertins chart	Proposed model
Air temp = -5	7-14 [cm/24 hour]	3.0 [cm/24 hour]
Air temp = -10	>15 [cm/24 hour]	8.0 [cm/24 hour]
Air temp = -15	>15 [cm/24 hour]	12.0 [cm/24 hour]

Appendix D

An example of simulation result

As an example of the simulation result, data set of the result of Case study 1 is shown. Upper half with 3103 structures are the calculation result of cylinder, rest of below half is for plate, each column means values for small structure elements. x-, y- and z- ; coordinate system of the each structural element by body fixed coordinate system of the ship. The right hand side row; 1-20 shows the ice load on the structure element on time domain along 20 hours operation. For cylinder those parameters are cylinder diameter and length, for plate it is area of the small element. KG and total ice load is calculated at the same time. For full data set see attached file.

Table D example of computation result, wind speed 14 [m/s], significant wave height 4.0 [m], air temperature -7 [°C] and computational duration is 20 hours.

structure number	X [m]	Y [m]	Z [m]	Diameter [m]	Length [m]	ice intensity [mm/hour]	Final ice Thickness [mm]	1	2	3	4	...	18	19	20
0	0.04	3.72	3.38	0.04	0.1	4.658	93.157	0.058	0.128	0.211	0.305		2.903	3.180	3.468
1	0.12	3.72	3.38	0.04	0.1	4.658	93.157	0.058	0.128	0.211	0.305		2.903	3.180	3.468
2	0.21	3.72	3.38	0.04	0.1	4.658	93.157	0.058	0.128	0.211	0.305		2.903	3.180	3.468
3	0.29	3.72	3.38	0.04	0.1	4.658	93.157	0.058	0.128	0.211	0.305		2.903	3.180	3.468
...															
3100	-22.5	0.41	3.08	0.04	0.1	4.669	93.381	0.058	0.129	0.212	0.306		2.915	3.193	3.483
3101	-22.5	0.41	3.18	0.04	0.1	4.666	93.313	0.058	0.129	0.211	0.306		2.911	3.189	3.478
3102	-22.5	0.41	3.28	0.04	0.1	4.662	93.238	0.058	0.129	0.211	0.306		2.907	3.184	3.473
3103	-22.5	0.41	3.38	0.04	0.1	4.658	93.157	0.058	0.128	0.211	0.305		2.903	3.180	3.468
KG								2.671	2.673	2.674	2.676		2.727	2.733	2.738
ice load								180.97	399.76	656.38	950.82		9044.62	9906.44	10806.07
				Area[m²]											
0	0	0	2.38	0.5		0.6359	12.718	0.283	0.566	0.849	1.132		5.093	5.376	5.659
1	0	0	2.48	0.5		0.6357	12.713	0.283	0.566	0.849	1.131		5.092	5.374	5.657
2	0	0	2.58	0.5		0.6354	12.707	0.283	0.565	0.848	1.131		5.089	5.372	5.655
3	0	0	2.68	0.5		0.6350	12.701	0.283	0.565	0.848	1.130		5.087	5.369	5.652
...															
77	0	0	10.08	0.5		0.4739	9.478	0.211	0.422	0.633	0.844		3.796	4.007	4.218
78	0	0	10.18	0.5		0.4708	9.415	0.209	0.419	0.628	0.838		3.771	3.980	4.190
79	0	0	10.28	0.5		0.4676	9.352	0.208	0.416	0.624	0.832		3.745	3.953	4.161
80	0	0	10.38	0.5		0.4644	9.288	0.207	0.413	0.620	0.827		3.720	3.927	4.133
KG								2.671	2.673	2.675	2.677		2.732	2.738	2.814
ice load [kg]								20.567	41.134	61.701	82.267		370.203	390.770	411.337
Total ice loads [kg]								201.53	440.89	718.08	1033.0		9414.82	10297.21	11217.41

61

Appendix E
C++ Source code

The C++ programming source code is shown here for the computation of ice load and following stability change. The source code is made by using "Microsoft Visual C++ Express edition".

```cpp
#include "stdafx.h"
#include <stdio.h>
#include <math.h>
#include <string.h>
#include <stdlib.h>
#define PI 3.141592653589

double ice_cylinder(double, double, double, double, double);        // define function "ice_cylinder"
double ice_plate(double, double, double, double, double);           // define function "ice_plate"
int red_superstructure(char [] , double **);

void main(){
        int n , i ,t , number_of_parts;
        double **superstruct, **superstruct_plate;
        double KG_height, drought, tonnage, density_ice, ice_r;
        double KG_resultant[20], KG_moment, mass_total, KG_moment_cylinder[20], mass_total_cylinder[20];
        double   icing_rate,
                        wind_speed,
                        ship_speed,
                        wave_height,
                        meas_height,
                        air_temp,
                        cylynder_diam;
        FILE *fp;
        char input_ship[128];

//********************** calculation for cylinder icing ********************

        //****   Secure Memories   *****************************
        superstruct = (double **)malloc(sizeof(double *)*10000);
        for(n=0;n<10000;n++)
                superstruct[n] = (double *)malloc(sizeof(double)*27);
        //************************************************
        icing_rate              = 0.0;
        wind_speed              = 14;
        ship_speed              = 0.0;
        wave_height             = 4.0;
        meas_height             = 2.0;
        air_temp                = -7.0;
        cylynder_diam           = 0.1;

        KG_height = 2.67;               //      meter, from keel, upward positive
        drought = 2.33;                 //      ship's drought
        tonnage = 420560.00;            //      ship's tonnage
        density_ice = 890.00;

        //****   Read ship super structure data      ***************
        input_ship[0] = '¥0';
        sprintf(input_ship,"ship_data_super.dat");
        fp = fopen(input_ship,"r");
        n=0;
        while((fscanf(fp,"%lf",&superstruct[n][0])) != EOF){
                for(i=1;i<27;i++)
                        fscanf(fp,"%lf",&superstruct[n][i]);
                n++;
        }
        fclose(fp);
        number_of_parts = n;
```

```c
//****************************************************
//====    superstruct profile        ===========================
//      superstruct[n][i];
//      n: number of structure
//      i=0: x coordinate
//      i=1: y coordinate
//      i=2: z coordinate
//      i=3: cylinder diameter
//      i=4: cylinder length
//      i=5: icing rate            (initially, =0)
//      i=6: ice thickness         (initially, =0)
//      i=7 : weight of ice at t=0 (initially, =0)
//      i=8 : weight of ice at t=1
//      i=9 : weight of ice at t=2
//      ...
//      i=26: weight of ice at t=19
//       (total 27 elements)
//==================================================

        fp = fopen("time_series.dat","w");
                for(n=0;n<number_of_parts;n++){
                        //****   Calculate icing rate        ***************
                        meas_height = superstruct[n][2];
                        cylynder_diam = superstruct[n][3];
                        icing_rate = ice_cylinder(wind_speed,ship_speed,wave_height,meas_height,air_temp);
                        superstruct[n][5] = icing_rate;
                        //****   Calculate ice thickness     ***************
                        for(t=7; t<27; t++){
                                superstruct[n][6] += icing_rate;
                                ice_r = cylynder_diam + superstruct[n][6]*0.001*2;
                                //****   Calculate ice weight       ***************
                                superstruct[n][t]             =             PI*0.25*(ice_r*ice_r            -
cylynder_diam*cylynder_diam)*superstruct[n][4]*density_ice;
                        }

                }
                //****    Calculate KG height      ***************

                        for(t=7;t<27;t++){
                                KG_moment = 0;
                                mass_total = 0;
                                for (n=0;n<number_of_parts;n++){

                                        KG_moment               =               KG_moment               +
(superstruct[n][2]+drought)*superstruct[n][t];
                                }
                                KG_moment_cylinder[t] = KG_moment;

                                for (n=0;n<number_of_parts;n++){
                                mass_total = mass_total + superstruct[n][t];
                                }
                                mass_total_cylinder[t] = mass_total;
                        KG_resultant[t] = ((KG_height*tonnage) + KG_moment) / (tonnage + mass_total);
                        }
                //******* output results                     ***************
                for (n=0;n<number_of_parts;n++){
                fprintf(fp,"%i     ",n);
                for(i=0;i<27;i++){
                        fprintf(fp,"%2.8f ",superstruct[n][i]);
                }
                        fprintf(fp,"\n");
                }
                fprintf(fp,"resultant KG is         ");

                for(t=7;t<27;t++){
                        fprintf(fp,"%f     ", KG_resultant[t]);
```

```c
                }

                fprintf(fp,"\n\n");
                //**********************************************
        fclose(fp);

        //****   Free Memories     ******************************
        for(n=0;n<10000;n++)
                free(superstruct[n]);
        free(superstruct);

//******************** calculation for plate icing ************************

        //****   Secure Memories   ***************************
        superstruct_plate = (double **)malloc(sizeof(double *)*1000);
        for(n=0;n<1000;n++)
                superstruct_plate[n] = (double *)malloc(sizeof(double)*26);
        //****************************************************

//****   Read ship super structure data for plate     ***************
        input_ship[0] = '\0';
        sprintf(input_ship,"ship_data_super_plate.dat");
        fp = fopen(input_ship,"r");
        n=0;
        while((fscanf(fp,"%lf",&superstruct_plate[n][0])) != EOF){
                for(i=1;i<26;i++)
                        fscanf(fp,"%lf",&superstruct_plate[n][i]);
                n++;
        }
        fclose(fp);
        number_of_parts = n;


        //****************************************************
        //====   superstruct_plate profile  =========================
        //      superstruct_plate[n][i];
        //      n: number of structure
        //      i=0: x coordinate
        //      i=1: y coordinate
        //      i=2: z coordinate
        //      i=3: plate area[m2]
        //      i=4: icing rate            (initially, =0)
        //      i=5: ice thickness         (initially, =0)
        //      i=6 : weight of ice at t=0 (initially, =0)
        //      i=7 : weight of ice at t=1
        //      i=8 : weight of ice at t=2
        //      ...
        //      i=25: weight of ice at t=19
        //       (total 26elements)
        //==================================================


        fp = fopen("time_series.dat","a");
                for(n=0;n<number_of_parts;n++){
                        //****   Calculate icing rate      ***************
                        meas_height = superstruct_plate[n][2];
                        icing_rate = ice_plate(wind_speed,ship_speed,wave_height,meas_height,air_temp);
                        superstruct_plate[n][4] = icing_rate;
                        //****   Calculate ice thickness    ***************
                        for(t=6;t<26;t++){
                                superstruct_plate[n][5] += icing_rate;
                                //****   Calculate ice weight      ***************
                                superstruct_plate[n][t]                                                      =
superstruct_plate[n][5]*0.001*superstruct_plate[n][3]*density_ice;
                        }

                }
                //****   Calculate KG height     ***************
                for(t=6;t<26;t++){
```

```c
                                KG_moment = 0;
                                mass_total = 0;
                                for (n=0;n<number_of_parts;n++){
                                        KG_moment                  =                  KG_moment                  +
(superstruct_plate[n][2]+drought)*superstruct_plate[n][t];
                                }
                                KG_moment = KG_moment + KG_moment_cylinder[t+1];
                                for (n=0;n<number_of_parts;n++){
                                        mass_total = mass_total + superstruct_plate[n][t];
                                }
                                        mass_total = mass_total + mass_total_cylinder[t+1];
                                KG_resultant[t] = ((KG_height*tonnage) + KG_moment) / (tonnage + mass_total);
                }
                        //****** output results                        ***************
                        for (n=0;n<number_of_parts;n++){
                        fprintf(fp,"%i    ",n);
                        for(i=0;i<26;i++){
                                fprintf(fp,"%2.8f ",superstruct_plate[n][i]);
                        }
                        fprintf(fp,"¥n");
                        }
                        fprintf(fp,"resultant KG is        ");

                        for(t=6;t<26;t++){
                                fprintf(fp,"%f    ", KG_resultant[t]);
                        }
                        fclose(fp);

                //****   Free Memories    *****************************
                for(n=0;n<1000;n++)
                        free(superstruct_plate[n]);
                free(superstruct_plate);
                //*****************************************************
}

//****************************** Horjen Ice Cylinder ***************************************
double ice_cylinder(double uu, double v, double hs, double z,double ta)
{

        double rw,a,ak, pi, gz, ggg, rice,b;

        pi= 3.1415926;                                                  // π
        rice = 890;                                                     // ice dencity
        ggg=9.81;                                                       // g
        rw=1025.0;                                                      // water dencity
        a=2.3489e-6;
        b=-2.0907;
        ak=12.077;

        gz = 1.7e-4 * hs * uu;

        //********* calculate droplet temperature **************
        float dd;
        double tau, ddd, cw, tw, ea, w, xt, lv, p, cp, ew, td, h;


        cw = 4000;                      // specific heat of water [J/kg.K]
        tau = 2.9;                      // duration of spray [sec]
        lv = 2.5e6;                     // latent heat of vaporization [J/kg]
        cp = 1005;                      // specific heat of air [J/kg.K]
        p = 100;                        // varometric pressure [kPa]
        h = 5.17 * exp(log(uu)*0.8);    // convective heat transfer coefficient [W/m2.k]
        rw = 1025;                      // water dencity [kg/m3]
        tw=0;
        dd= 0.001;                      //droplet diameter [mm]
        ddd=0.4;                        // characteristic length [m]
```

65

```
        ea = 1.9226e-7*ta*ta*ta*ta + 2.4545e-5*ta*ta*ta + 1.4224e-3*ta*ta + 0.044436*ta + 0.61094;

        w = tw;
        while(1){
                ew = 1.9226e-7*w*w*w*w + 2.4545e-5*w*w*w + 1.4224e-3*w*w + 0.044436*w + 0.61094;
                xt = 1 + 0.622*lv/p/cp*(ea-ew)/(ta-w);                                      // X_theta
        td = ta + (w-ta)*exp(-0.2514*h*ddd/(rw*cw*dd*dd) * xt * tau);
                if (fabs(w-td)<0.00001)
                            break;
                else
                            w = td;
        }

// computation of freezing fraction "n"
        float tf, ss;
        double ts, es, mi, n, nn;

        ss = 35;                                        // salinity of sea water [ppt]
        tf = -0.002 -0.0524 * ss -6e-5*ss;

        n=0;
        while(1){
                ts = (1 + n)*tf;
                es = 1.9226e-7*ts*ts*ts*ts + 2.4545e-5*ts*ts*ts + 1.4224e-3*ts*ts + 0.044436*ts + 0.61094;
                mi = hs*uu*(ts-td) + h*(ts-ta) + 89.5*exp(log(uu)*0.8)*(es-ea);
                nn = mi/lv/gz;
                if (fabs(nn-n)<0.00001) break;
                n=nn;

        }

        double nnn;

        nnn = nn*gz/rice*3.6e6;

    return nnn;
}


//***************************** Horjen Ice plate ***********************************
double ice_plate(double uu, double v, double hs, double z,double ta)
{

        double rw,a,ak, pi, gz, ggg, rice, b, ddd;

        pi= 3.1415926;                          // π
        rice = 890;                             // ice density
        ggg=9.81;                               // g
        rw=1025.0;                              // water density
        a=2.3489e-6;
        b=-2.0907;
        ak=12.077;
        gz = 1.7e-4 * hs * uu;

        //*********** calculation for droplet temperature ***************
        float dd;                               // droplet diameter, characteristic length [m]
        double tau, cw, tw, ea, w, xt, lv, p, cp, ew, td, h;

        cw = 4000;                                              // specific heat of water [J/kg.K]
        tau =2.9;                                               // duration of spray [sec]
        lv = 2.5e6;                                             // latent heat of vaporization [J/kg]
        cp = 1005;                                              // specific heat of air [J/kg.K]
        p = 100;                                                // barometric pressure [kPa]
        ddd = 0.4;                                              // characteristic length [m]
        h = 6.3279 * exp(log(uu)*0.8) / exp(log(ddd)*0.2);      // convective heat transfer coefficient [W/m2.k]
        rw = 1025;                                              // water density [kg/m3]
        tw = 0;
```

```c
        dd = 0.001;                                          // droplet diameter [mm]

        ea = 1.9226e-7*ta*ta*ta*ta + 2.4545e-5*ta*ta*ta + 1.4224e-3*ta*ta + 0.044436*ta + 0.61094;

        w = tw;
        while(1){
                ew = 1.9226e-7*w*w*w*w + 2.4545e-5*w*w*w + 1.4224e-3*w*w + 0.044436*w + 0.61094;
                xt = 1 + 0.622*lv/p/cp*(ea-ew)/(ta-w);                  // X_theta
                td = ta + (w-ta)*exp(-0.2514*h*ddd/(rw*cw*dd*dd) * xt * tau);
                if (fabs(w-td)<0.00010)
                        break;
                else
                        w = td;
        }

// computation of freezing fraction "n"
        float tf, ss;
        double ts, es, mi, n, nn;

        ss = 35;                                             // salinity of sea water [ppt]
        tf = -0.002 -0.0524 * ss -6e-5*ss;

        n=0;
        while(1){
                ts = (1 + n)*tf;
                es = 1.9226e-7*ts*ts*ts*ts + 2.4545e-5*ts*ts*ts + 1.4224e-3*ts*ts + 0.044436*ts + 0.61094;
                mi = hs*uu*(ts-td) + h*(ts-ta) + 89.5*exp(log(uu)*0.8)*(es-ea);
                nn = mi/lv/gz;
                if (fabs(nn-n)<0.0001) break;
                n=nn;
        }

// final computation result which is icing intencity
        double nnn;

        nnn = nn*gz/rice*3.6e6;

    return nnn;
}
```